

# Lick Northern Proper Motion Program. III. Lick NPM2 Catalog

Robert B. Hanson, Arnold R. Klemola, and Burton F. Jones

*University of California Observatories/Lick Observatory,  
University of California, Santa Cruz, CA 95064*

`hanson,klemola,jones@ucolick.org`

and

David G. Monet

*US Naval Observatory, Flagstaff Station, P.O. Box 1149, Flagstaff, AZ 86002*

`dgm@nofs.navy.mil`

## ABSTRACT

The Lick Northern Proper Motion (NPM) program, a two-epoch (1947–1988) photographic survey of the northern two-thirds of the sky ( $\delta \gtrsim -23^\circ$ ), has measured absolute proper motions, on an inertial system defined by distant galaxies, for 378,360 stars from  $8 \lesssim B \lesssim 18$ . The 1993 NPM1 Catalog contains 148,940 stars in 899 fields outside the Milky Way’s zone of avoidance. The 2003 NPM2 Catalog contains 232,062 stars in the remaining 347 NPM fields near the plane of the Milky Way. This paper describes the NPM2 star selection, plate measurements, astrometric and photometric data reductions, and catalog compilation. The NPM2 Catalog contains 122,806 faint ( $B \geq 14$ ) anonymous stars for astrometry and galactic studies, 91,648 bright ( $B < 14$ ) positional reference stars, and 34,868 “special stars” chosen for astrophysical interest. The NPM2 proper motions are on the ICRS system, via Tycho-2 stars, to an accuracy of  $0.6 \text{ mas yr}^{-1}$  in each field. RMS proper motion precision is  $6 \text{ mas yr}^{-1}$ . Positional errors average 80 mas at the mean plate epoch 1968, and 200 mas at the NPM2 catalog epoch 2000. NPM2 photographic photometry errors average 0.18 mag in  $B$ , and 0.20 mag in  $B - V$ . The NPM2 Catalog and the updated (to J2000) NPM1 Catalog are available at the CDS Strasbourg data center and on the NPM WWW site<sup>1</sup>. The NPM2 Catalog completes the Lick Northern Proper

---

<sup>1</sup><http://www.ucolick.org/~npm>

Motion program after a half-century of work by three generations of Lick Observatory astronomers. The NPM Catalogs will serve as a database for research in galactic structure, stellar kinematics, and astrometry.

*Subject headings:* astrometry, catalogs

## 1. Introduction

The study of the motions of various classes of stars is fundamental to an understanding of our Galaxy. Proper motions provide the observational basis for the study of solar motion, galactic rotation, and stellar velocity dispersions, and for the statistical determination of stellar distances and luminosities. The Lick Northern Proper Motion (NPM) program (Klemola, Jones, & Hanson 1987, Paper I), a two-epoch photographic survey of the northern two-thirds of the sky, now complete after a half-century of work, meets many of these basic observational needs by measuring absolute proper motions on an inertial system defined by distant galaxies, accurate positions, and *BV* photographic photometry for 378,360 stars over a blue apparent magnitude range from 8 to 18.

The NPM program includes many types of stars chosen for astrophysical interest, anonymous stars for astrometry and galactic studies, and a selection of stars from positional catalogs and from other proper motion surveys. The NPM survey consists of 1,246  $6^\circ \times 6^\circ$  fields with  $\delta \gtrsim -23^\circ$  photographed with the Lick 51 cm (20 in) Carnegie double astrograph (scale  $\sim 55''.1 \text{ mm}^{-1}$ ) at two epochs (1947–1954 and 1970–1988). Paper I describes the Lick astrograph and plate material, and gives a comprehensive overview of the history, goals, and methods of the NPM program.

The main results of the Lick NPM program (positions, proper motions, magnitudes, and colors) are published in two catalogs, the NPM1 Catalog (Klemola, Hanson, & Jones 1993a) with 148,940 stars in 899 “NPM1” fields outside the Milky Way’s zone of avoidance, and the NPM2 Catalog (Hanson et al. 2003), with 232,062 stars in the remaining 347 “NPM2” fields near the plane of the Milky Way. Figure 1 shows the sky distribution of the NPM1 and NPM2 fields. As a service to users, the 1993 NPM1 Catalog has been updated (Klemola, Hanson, & Jones 2000) from the obsolete B1950 coordinates to the J2000 epoch and equinox used for NPM2. The two NPM Catalogs and associated documentation files are available from the CDS Strasbourg data center and on the Lick NPM program’s WWW site <http://www.ucolick.org/~npm>.

Several products supplementing the NPM Catalogs have also been compiled. The Lick Input Catalog of Special Stars (ICSS; see Paper I) represents Klemola’s continuing search

of the astronomical literature since 1972 to include many classes of stars of astronomical or astrophysical interest in the NPM program. Klemola’s ICSS now contains some 300,000 entries for 220,000 stars from over 1,100 literature references, and forms the basis for two published catalogs. The NPM1 Cross-Identifications (Klemola, Hanson, & Jones 1994) contains 41,858 entries with source identifications, stellar type classifications, publication references, footnotes, and other information to assist users of the NPM1 Catalog. The NPM2 Cross-Identifications (Klemola et al. 2004), with 46,887 entries, is the corresponding supplement to the NPM2 Catalog. Another supplement to NPM1 is the NPM1 Reference Galaxies list (Klemola, Hanson, & Jones 1993b), giving  $0''.2$  precision positions and  $B$  magnitudes for 50,517 faint galaxies (mostly  $16 \lesssim B \lesssim 18$ ) used as the proper motion reference frame for NPM1.

The ultimate goal of the NPM program, in coordination with the Yale Southern Proper Motion (SPM) program (Girard et al. 1998; Platais et al. 1998a; Girard et al. 2004) is to provide accurate absolute proper motions for faint stars ( $B \gtrsim 12$ ) over the whole sky, on a reliable, uniform system, linked (Kovalevsky et al. 1997; Platais et al. 1998b) to the ICRS/Hipparcos (ESA 1997) proper motion frame realized by bright stars ( $B \lesssim 12$ ). The scientific significance of the Lick NPM program is that its large size, extensive magnitude range ( $8 \lesssim B \lesssim 18$ ), high accuracy, and absolute proper motions will ensure its lasting value as a unique database for research in galactic structure and kinematics (Hanson 1987; Beers et al. 2000), stellar luminosities (Layden et al. 1996) and astrometry (Platais et al. 1998b).

Klemola, Hanson, & Jones (1995) and Hanson (1997) have described the NPM1 Catalog and its applications. This paper will describe the NPM2 Catalog, including details of the NPM2 star selection, astrometric and photometric data reductions, and catalog compilation. We will emphasize the differences between NPM2 and NPM1, and compare the characteristics of both catalogs. The reader should be aware that the NPM2 plate material, the general structure of the astrometric and photometric data reduction “pipeline”, and much of the NPM2 catalog compilation procedures and error tests are essentially similar to NPM1. Details not mentioned in this paper are as described in Paper I (plate material, reduction procedures), or in Klemola, Hanson, & Jones (1995) and Hanson (1997) (catalog compilation and contents). The most important differences between NPM2 and NPM1 are:

1. For NPM2, the Lick astrograph plates were scanned by the Precision Measuring Machine (PMM) at the US Naval Observatory, Flagstaff (Section 2.2). Stars selected for NPM2 were identified and extracted from the PMM scans (Section 2.3). For NPM1, the plates were measured on the Automatic Measuring Engine (AME) at Santa Cruz, using an input list of stars previously selected at the Lick Survey Machine.
2. With the PMM scans, NPM2 could use many more reference stars than NPM1 in the

astrometric and photometric data reductions (Sections 4, 5, and 6). This allowed more rigorous plate constant models and more robust reductions.

3. NPM2 fields lie in the zone of avoidance, and have far too few galaxies to determine the zero-point corrections from relative to absolute proper motion as per NPM1. For NPM2, we used Tycho-2 Catalogue (Høg et al. 2000a,b) stars to correct each field’s relative proper motions to the ICRS system (Section 5).

Section 2 describes how the different classes of stars were selected for NPM2, briefly discusses the PMM scans of the NPM plates, and explains how the  $X, Y$  and magnitude measurements for NPM2 stars were extracted from the PMM scans. Section 3 outlines the NPM2 data reductions, describes the selection of astrometric reference stars, and discusses the astrometric modeling of the Lick astrograph plates. Sections 4, 5, and 6 explain the NPM2 astrometric (positions and proper motions) and photometric ( $B$  magnitude,  $B-V$  color) reductions and internal error tests. Section 7 tells how the NPM2 Catalog was compiled. Multiple measures from the 347 overlapping fields were averaged, checked for discordances, and used to estimate the accuracy of the NPM2 positions, proper motions, and photometry. We outline the organization of the NPM2 Catalog, and discuss the NPM2 Cross-Identifications. Finally, Section 8 summarizes the NPM program and outlines present or potential applications of the NPM data to galactic research.

## 2. Star Selection and Plate Measurement

For NPM1, the selection of stars in each field and the measurement of the plates were two separate processes, described in Section IV of Paper I. NPM2 is more complicated. For the most part, broad categories of stars desired for NPM2 were defined in advance, but the specific stars were chosen *a posteriori* when the data were extracted from the PMM scans.

### 2.1. NPM2 Stellar Content

The stellar content of the NPM1 Catalog, including Klemola’s ICSS, was detailed in Paper I. The content of the NPM2 Catalog is broadly similar to NPM1, with the major additions discussed below, and other differences described by Hanson (1997), most notably Klemola’s continued updating of the ICSS. Six broad categories of stars selected for the NPM program are outlined in Table 1. NPM2 selected about four times as many stars per field as NPM1. The main reasons are:

1. To improve our proper motion reductions (Section 5), and to provide a denser network (10 stars  $\text{deg}^{-1}$ ) of faint ( $B \gtrsim 16$ ) stars with accurate positions, NPM2 selected over 400 faint anonymous stars per field, compared to 72 or 144 for NPM1.
2. NPM2 includes large numbers of stars from Hipparcos, Tycho, and other catalogs not available to NPM1. Most notably, NPM2 includes  $\sim 400$  astrometric reference stars per field from the 2.5-million-star Tycho-2 Catalogue (Høg et al. 2000a,b), greatly improving the accuracy of our positional reductions (Section 4).
3. Many classes of stars are concentrated to the galactic plane or toward the galactic center, so the average sky density for NPM2 is much higher than for NPM1. About 55% of Klemola’s ICSS, some 123,000 stars, fall into the 347 NPM2 fields.<sup>2</sup> Abundant ICSS classes that show strong concentration to the Milky Way include 7000 OB stars, 5000 red giants, 3000 carbon stars, and 2000 RR Lyrae type variable stars.
4. Klemola’s literature surveys continually added stars to the ICSS, which is now four times as large as the version used for NPM1. Table II of Paper I lists the major classes of stars in Klemola’s ICSS. The ICSS also includes large numbers of stars from two-color and objective-prism surveys, and many stars from recent surveys of the galactic anticenter and elsewhere. Several major catalogs or compilations are now included whole in the ICSS. These include the GCVS4 (Kholopov et al. 1998) variable star catalog with its supplements, the new Yale Parallax Catalogue (van Altena, Lee, & Hoffleit 1995), the Third Catalogue of Nearby Stars (Gliese & Jahreiss 1991), and the NLTT proper motion catalog (Luyten 1979). These additions will greatly enhance the body of basic data for galactic studies.

In total, the NPM2 Catalog (Section 7) contains 122,806 faint anonymous stars selected for the NPM2 astrometric reductions and for statistical studies of stellar motions; 91,648 positional reference stars, mostly from the Tycho-2 Catalogue; and 34,868 “special stars” from Klemola’s ICSS. These categories overlap slightly; the final NPM2 Catalog (Section 7) totals 232,062 stars from all 347 NPM2 fields.

---

<sup>2</sup>As discussed in Section 7.4, only about 30% of these ICSS stars “survive” in the NPM2 Catalog. Star counts cited here are ICSS counts. Section 7.3 gives NPM1 + NPM2 Catalog counts for several major stellar classes.

## 2.2. PMM Scans

From September 1996 to January 1999, under the supervision of Monet, a total of 3,882  $17 \times 17$  in plates, essentially the entire NPM plate collection, was scanned with the Precision Measuring Machine (PMM; Monet et al. 2003) at the US Naval Observatory, Flagstaff. This includes the 899 fields previously measured at Lick for NPM1, as well as the 347 NPM2 fields. There are three plates per NPM field: blue at first epoch (“B1”), blue (“B2”) and yellow (“Y2”) at second epoch. (For completeness, PMM also scanned 144 B1 plates in the two Southern Extension zones (centers at  $\delta = -25^\circ$  and  $-30^\circ$ ), which were photographed at Lick in the 1950s but not repeated for the NPM program.) The operation of the PMM and the reduction of the pixel data (transmission values) to  $X, Y$  coordinates and instrumental magnitudes ( $m_b$  or  $m_y$ ) were as described by Girard et al. (2004) for the SPM program. Plates were scanned in the “direct” orientation only.

Positional and photometric data for all images detected (up to  $3.4 \times 10^6$  per plate) were saved on 207 CD-ROMs, comprising  $\sim 130$  Gb of data for further analysis. Data for the 347 NPM2 fields were extracted for astrometric and photometric reductions. Many other uses of the NPM plate scan database are possible, such as expanding the NPM1 Catalog, or making all-sky catalogs beyond the limited scope of the NPM program (Monet et al. 2003).

The completion of the NPM plate scans at Flagstaff, with a new generation of measuring machine, truly represents a remarkable increase in speed; by comparison, it took 17 years to survey and measure the 899 NPM1 fields on the Lick AME at Santa Cruz.

The NPM2 plate reductions (Secs. 4, 5, and 6) verified that the positional ( $1\text{--}2 \mu\text{m} \simeq 50\text{--}100$  mas) and photometric ( $\sim 0.2$  mag) precision of PMM on the NPM plates are quite comparable to the Lick AME (Paper I) when oversize, weak, or blended images are excluded from the data reduction pipeline, which we took considerable effort to do for NPM2. This allows the NPM2 Catalog, from PMM scans, to be as precise as what we achieved for NPM1 from AME measurements.

## 2.3. NPM2 Star Image Data Extraction

The main purpose of the NPM program (Paper I) is to establish a reference frame and determine absolute proper motions for stars of astrophysical or kinematical interest, not to measure every star on the plates. Here we describe how we selected from the PMM scans (averaging  $\sim 10^6$  image detections per NPM2 plate) those stars (and image combinations) we wanted for NPM2. This task is complicated by the fact that the Lick plates have two exposures (I = long; II = short) and were taken with parallel-wire objective gratings. (See

Section IVa of Paper I and Section III of Klemola et al. (1971) for details.) Bright stars ( $B \lesssim 14$ ) have many images, most of which are not useful for astrometry, and many of which may overlap with other stars’ images in the dense NPM2 fields. Besides extracting the  $X, Y$  coordinates and  $m_b$  or  $m_y$  instrumental magnitudes, the exposure system (I or II) and grating order (0, 1, 2, or 3) of each image must be recognized.

On the Lick plates, only those system/order combinations known (from NPM1) to give good astrometry were selected from the PMM scans. For faint stars ( $B \gtrsim 14$ ), only the long-exposure I(0) image is useful. For stars with  $B \lesssim 14$ , we use I(2), I(3), and II(0) on the blue plates; I(1), I(2), and II(0) on the yellow plates. Grating images are always taken as north-south pairs for orders 1, 2, or 3. For the brightest stars ( $B \lesssim 10$ ), only the short-exposure II(0) image is useful. The task of selecting NPM2 stars from the PMM scans divided into three parts:

1. For most NPM2 stars, image selection could be done automatically, i.e. without first having to identify the stars at the Lick Survey Machine (as was done for all stars in NPM1). Stars with known, accurate positions, chiefly bright ( $B \lesssim 13$ ) stars from Hipparcos, Tycho-2, and other astrometric catalogs, could be identified once a transformation was established, for each plate, between  $\alpha, \delta$  and  $X, Y$  on the PMM scans. We developed software, based partly on Yale SPM programs (Girard et al. 2004), to automate the process of extracting these stars’ useful images (or image systems) from the PMM scans.
2. Faint anonymous astrometric reference stars (400 per field for NPM2), were also selected automatically. We identified unblended I(0) images with  $15 \lesssim B \lesssim 17$ , uniformly distributed over each field. To ensure choosing the same star on all three plates (B1, B2, Y2), stars with proper motion displacements ( $B2 - B1$  or  $Y2 - B1$ ) larger than  $\sim 30 \mu\text{m}$  were not selected.
3. All NPM2 stars not already having accurate positions were identified at the Lick Survey Machine (often using finding charts). Klemola surveyed all 347 NPM2 fields to provide the  $X, Y$  coordinates that allowed these stars’ images to be selected from the PMM scans. Most of the fainter ( $B \gtrsim 12$ ) “special stars” chosen from the literature by Klemola for their astronomical interest fell into this category. Conservative procedures were followed to avoid erroneous selections. About 6% of surveyed stars were not selected from the B1 plate scans; another 4% were “lost” on the B2 plate scans.

For each NPM2 field, every star selected was indexed for cross-identification, and the data from the PMM scans for each plate (B1, B2, Y2) were organized into the same file

structure used for NPM1, allowing the PMM data to enter the NPM data reduction pipeline originally designed for AME plate measurements.

### 3. NPM2 Data Reductions

Wide-field astrograph plates such as those of NPM and SPM are a unique astrometric resource because they are amenable to the techniques of differential astrometry necessary to determine accurate absolute proper motions (Paper I; Platais et al. 1998a), and can be measured with astrometric precision over a magnitude range ( $8 \lesssim B \lesssim 18$  for NPM;  $5 \lesssim V \lesssim 18$  for SPM) wide enough to encompass bright astrometric reference stars *and* faint galaxies. Accurate astrometry is greatly facilitated when plates of a field at multiple epochs can be closely “matched” (plate center, hour angle, emulsion, exposure, etc.) in a way that can be achieved with a dedicated, stable telescope such as the Lick astrograph. With well-matched plates and differential reductions, image irregularities and magnitude-dependent effects have minimal impact on the proper motions. The NPM2 data reductions are designed to work differentially whenever possible, to take fullest advantage of the Lick astrograph plates.

To optimize accuracy, we have repeatedly tested and refined the procedures and plate models for determination of positions, proper motions, magnitudes, and colors using the NPM plates. For NPM2 we extensively revised the NPM1 reduction programs (Sections VI and VII of Paper I), with more sophisticated plate models and rapid automated checking to delete blended images and erroneous measurements. References to Paper I will mark procedures that are still the same as for NPM1. The structure of the NPM2 reductions is much the same as NPM1: Each field is reduced independently. Each step in the astrometric and photometric reductions of the B1, B2, and Y2 plates (or plate pairs; see below) produces plate constants, which are later used to transform the  $X, Y$  plate coordinates<sup>3</sup> and  $m_b, m_y$  instrumental magnitudes into positions, proper motions,  $B$  magnitudes, and  $B-V$  colors. To avoid spurious results, discordant or doubtful measures noted at any stage of the reductions are rejected. (Rejections average 5% on blue plates, 3% on yellow.) Finally, multiple measures of any star are checked and averaged to give one entry per star (J2000 position at mean plate epoch  $\sim 1968$ , absolute proper motion,  $B$  magnitude, and  $B-V$  color). The result is a set of 347 “field catalogs”, which were compiled into the NPM2 Catalog as described in Section 7.

---

<sup>3</sup>The NPM2 reductions use  $X, Y$  coordinates in mm, with the origin at the plate center.  $X, Y$  residuals will be expressed in  $\mu\text{m}$ .



### 3.1. Reference Stars

NPM2 was able to use more sophisticated plate models than NPM1 because (1) the PMM data are full plate scans, supplying many more potential reference stars than NPM1, which was limited to the stars pre-selected for AME measurement; and (2) the release of the Tycho-2 Catalogue in 2000 greatly increased the numbers of stars faint enough ( $B > 8$ ) to be useful to NPM2 that have accurate positions, proper motions, and photometry. Using more reference stars enabled major improvements in all three phases of the NPM2 reductions.

The two-exposure NPM photography optimized image quality for “bright” stars ( $B \sim 12$ ) and “faint” stars ( $B \sim 16$ ). For the proper motion reductions, stars with  $15 \lesssim B \lesssim 17$  are so abundant that we could take as many as needed (400 per field) from the PMM scans (Section 2.3). However, an ideal positional reference frame for the NPM plates at  $11 \lesssim B \lesssim 13$  would extend at least 1 mag fainter than the ACRS Catalog (Corbin, Urban, & Warren 1991), which we used for NPM1.

Tycho-2 is nominally complete only to  $V_T \sim 11$ , but it actually contains nearly 1.7 million stars with  $V_T > 11$  (see Table 2 of Høg et al. 2000b), with moderately accurate positions ( $60 < \sigma < 90$  mas) and proper motions ( $2.5 < \sigma < 3$  mas yr<sup>-1</sup>) in the ICRS/Hipparcos system, and two-color ( $B_T, V_T$ ) photometry ( $0.1 < \sigma < 0.3$  mag). Switching to Tycho-2 as our positional reference catalog allowed us to use as many stars as necessary, in the ideal magnitude range, to model the NPM2 plates for the highest possible positional accuracy. From the PMM scans, we extracted 200 Tycho-2 stars distributed uniformly over each field, in the magnitude range  $11 < B_T < 13$ , in addition to a roughly equal number of (generally brighter) Tycho-2 stars already chosen for other reasons.

### 3.2. Astrometric Plate Model

Having some 400 Tycho-2 reference stars allows the NPM2 positional reductions to use the same cubic plate model as the proper motion reductions. This desirable consistency had not been possible for NPM1, where having only  $\sim 50$  ACRS reference stars per field (see Table 1) limited the positional plate model to a five-constant quadratic in each coordinate, and required pre-corrections for cubic radial distortion. Using the *same* astrometric model consistently for positions *and* proper motions also has the advantage that the two reductions can be compared, for example to check whether  $(X, Y)$ -dependent effects seen in the position reductions are also evident in the proper motions (see below, and Section 5.2).

The NPM2 astrometric plate model (Table 2), optimized after extensive test reductions, is a minor improvement on the 13-constant model we used for the NPM1 proper motion

reductions (Section VIIa of Paper I). These models represent a sophisticated compromise between (1) a simple “physical” model with seven terms for zero point  $(X, Y)$ , scale, rotation, plate tilt  $(P, Q)$ , and cubic radial distortion; and (2) a full cubic model with separate terms in in each coordinate ( $2 \times 10 = 20$  terms). We can render several of these terms unnecessary by pre-correcting the  $X, Y$  measures for differential aberration and refraction (König 1962, Eqs. 20 and 25).

With a full cubic plate model, high correlations ( $\rho > 0.9$ ) between the linear and cubic terms are always present. NPM1 showed that these correlations can be substantially reduced (to  $\sim 0.7$ ) by tying together the  $X$  and  $Y$  solutions by a common scale coefficient, which is possible when differential refraction is pre-corrected. Moreover, several terms ( $Y^2$  and  $Y^3$  in  $X$ ;  $X^2$  and  $X^3$  in  $Y$ ) with no clear physical significance proved to be negligible in test reductions, and could be eliminated from the model.

With 400 reference stars per NPM2 field, we can determine a full set of cubic distortion terms ( $X^3$  and  $XY^2$  in  $X$ ;  $X^2Y$  and  $Y^3$  in  $Y$ ) on each plate (positions) or plate pair (proper motions) instead of the fixed radial-distortion pre-corrections NPM1 used. Finally, we now solve for the diagonal distortion-like cubic term ( $X^2Y$  in  $X$ ;  $XY^2$  in  $Y$ ) discovered in NPM1.

The NPM2 plate model (Table 2) has 14 terms, one more than the NPM1 proper motion model. The terms in the NPM2 model that would be equal in a simple seven-constant physical model are those for rotation ( $c_2 = c_3$ ), plate tilt ( $c_6 = c_8 = P$ ,  $c_7 = c_9 = Q$ ), and radial distortion ( $c_{10} = c_{11} = c_{12} = c_{13}$ ). In the NPM2 reductions, these terms usually show small but significant differences, because they absorb unmodeled effects such as higher-order or radially-asymmetric distortion.

For the most part, the numerical values of the position and proper motion plate constants have little scientific importance, tending simply to reflect the circumstances of observation and measurement. However, three points regarding the cubic terms are worth noting: (1) The NPM2 distortion constants are quite small (mean size  $\lesssim 10^{-9}$  mm $^{-2}$ , amounting to 10–20  $\mu$ m at the plate edges and corners), but highly significant (usually 5–10  $\sigma$ ). This is like what Platais et al. (1995) found for the SPM plates, but we find no significant trends of the NPM2 constants over time. (2) Mean values of the NPM2 constants nearly equal the values adopted in the NPM1 position reductions or determined in the NPM1 proper motion reductions. (3) Field by field, the *differences* between the NPM2 B1 and B2 position constants roughly equal the the corresponding proper motion plate constants determined by differential reduction of the B1 and B2 plates.

We note that the NPM2 plate model does *not* include magnitude-dependent terms. For positions, the magnitude range ( $9 < B < 13$ ) of the Tycho-2 reference stars is not large

enough to determine such terms reliably on each plate (B1, B2, Y2). Moreover, there is no reason to expect that the *same* terms would apply to the faint stars ( $14 < B < 18$ ) that form the bulk of the NPM program. The possibility of magnitude-dependent corrections to the NPM2 positions is considered in Section 4.5. For proper motions, we use faint anonymous stars ( $15 \lesssim B \lesssim 17$ ) on each (B1, B2) plate pair. Magnitude terms cannot be used in the plate solutions because such terms would absorb real effects (e.g., secular parallaxes) in the stellar motions. Magnitude-dependent systematic proper motion errors for our bright stars ( $8 < B < 12$ ) are corrected in each field as part of the final correction from relative to absolute proper motions, discussed in Section 5.4.

## 4. Positional Reductions

For each of the 347 NPM2 fields, the reduction of the PMM  $X, Y$  measures to J2000 positions  $\alpha, \delta$  is done in four stages. Until the final stage, all three plates (B1, B2, and Y2) are reduced separately, as follows.

### 4.1. Bridge Reductions and Pre-Corrections

As in NPM1 (Section VIa of Paper I), the first step in the NPM2 plate reductions is the positional “bridge reduction”, which differentially reduces bright stars’ short-exposure images into the  $X, Y$  system of the long exposure. First, on each plate, all (north-south) diffraction-grating image pairs  $I(\text{gr})$  are averaged. The average is equivalent to the  $I(0)$  position<sup>4</sup>, neglecting small magnitude- and color-dependent effects (see Section 4.5). Then, all stars having  $I(\text{gr})$  and  $II(0)$  images (usually over 200 stars on B1 and B2, near 400 on Y2; 4–6 times as many as NPM1) are identified. As in NPM1, the  $II(0)$  images are corrected for differential plate tilt, so that a simple four-constant solution (scale, rotation, and  $X, Y$  zero point) can transform all  $II(0)$   $X, Y$  measures on the plate to the  $I(0)$  system. The unit weight errors of the bridge solutions are generally 3–4  $\mu\text{m}$  on B1 and B2, and 2  $\mu\text{m}$  on Y2. These are about twice the PMM  $X, Y$  errors, largely because many poor (e.g. weak, overexposed, or blended) images have not yet been rejected.) The contribution of the bridge transformation to the positional error for a bright star’s  $II(0)$  image is very small, about 12–16 mas on B1 and B2, and 6 mas on Y2.

---

<sup>4</sup>The SPM (Girard et al. 1998, 2004) procedure, which explicitly reduces grating images to the zero-order system, cannot be used on the NPM plates, where the  $I(\text{gr})$  and  $I(0)$  images are never useful for the same star.

Next, multiple measures of one star are checked for consistency of position. Stars with discordant  $X, Y$  measures (more than  $5 \mu\text{m}$  from the mean) are examined to identify which image system should be rejected. If that fails (e.g., when there are only two measures) the star is totally rejected. Generally, 1-2% of all images are rejected here; most of these are blended images not recognized at the PMM star selection stage.

After the bridge reduction, all the  $X, Y$  measures on the plate, for bright and faint stars alike, are on the I(0) system of the faint stars. Finally, we pre-correct  $X, Y$  for differential aberration and refraction, as in NPM1. The reduced  $X, Y$  values for each plate (B1, B2, Y2) are then used as input to the plate-constant reductions for positions and proper motions.

## 4.2. Plate Constant Reductions

All positional reference stars used for NPM2 come from the Tycho-2 Catalogue, which lists mean positions and proper motions in the ICRS system. Tycho-2 positions are given for the catalog epoch J2000, with the Tycho-2 proper motions having been used to propagate the positions from the mean observational epoch  $T_0$  (averaging  $\sim 1980$  but ranging from  $\sim 1912$  to  $\sim 1992$ ) to the J2000 epoch. Position errors  $\sigma_0$  in each coordinate are given at the mean epoch  $T_0$ , where position and proper motion are uncorrelated, and the positional error is minimized. These data are sufficient to propagate the Tycho-2 positions and their errors to any other epoch.

For each NPM2 plate (B1, B2, Y2), we backdate the Tycho-2 positions (J2000 coordinates and epoch) to the Lick plate epoch  $T_1$  (near 1950 for B1; usually 1970–1980 for B2, Y2) using the Tycho-2 proper motions. In each coordinate the Tycho-2 position error  $\sigma_1$  at the Lick plate epoch is the quadratic sum of the pure positional error ( $\sigma_0$ ) and the proper motion error ( $\sigma_\mu$ ) accumulated over  $|T_1 - T_0|$  years:

$$\sigma_1^2 = \sigma_0^2 + \sigma_\mu^2 (T_1 - T_0)^2. \quad (1)$$

The errors  $\sigma_1$  of the backdated Tycho-2 positions used for NPM2 average  $\sim 90$  mas ( $1.6 \mu\text{m}$  on the NPM plates) at the Lick first epoch, and  $\sim 60$  mas ( $1.1 \mu\text{m}$ ) at the second epoch. This is roughly the size of the PMM measurement errors.

On each plate, the backdated Tycho-2 positions are used to compute standard coordinates  $X_T, Y_T$  (in millimeters from the plate center) for each star. The PMM measures for each Tycho-2 star are averaged over multiple image systems if necessary. The measured coordinates  $X_M, Y_M$  are then adjusted to the standard coordinates in a least-squares solution with the equations of condition

$$\Delta X = X_T - X_M = \sum_{i=1}^{14} c_i T_{i,X} \quad (2a)$$

and

$$\Delta Y = Y_T - Y_M = \sum_{i=1}^{14} c_i T_{i,Y} \quad (2b)$$

where  $c_i$  are the 14 plate constants and  $T_{i,X}$ ,  $T_{i,Y}$  are the corresponding  $X, Y$  terms in Table 2, evaluated using  $X_M, Y_M$ . Terms not used in  $X$  have  $T_{i,X} = 0$ ; likewise for  $Y$ . We define the  $\Delta X$  and  $\Delta Y$  differences as “catalog minus measured”, to be consistent with NPM1. Weights are determined from the Tycho-2 errors (Eq. 1) and nominal values of the PMM measurement errors. Each star’s residuals are

$$R_X = X_T - X_S = X_T - (X_M + \Delta X), \quad (3a)$$

and

$$R_Y = Y_T - Y_S = Y_T - (Y_M + \Delta Y), \quad (3b)$$

where  $X_S, Y_S$  are the standard coordinates corresponding to  $X_M, Y_M$ . Stars with large residuals are rejected and the solutions repeated. After convergence, the numbers of Tycho-2 stars surviving average 350 per blue plate, and 390 per yellow plate.

Over all 347 NPM2 fields, the RMS unit weight errors  $\sigma_{pos}$  of the position solutions are  $3.5 \mu\text{m}$  (190 mas) for B1 plates,  $2.9 \mu\text{m}$  (160 mas) for B2, and  $1.8 \mu\text{m}$  (100 mas) for Y2. The differences chiefly reflect that the Lick yellow plates have sharper images, and the Tycho-2 positions are generally more accurate near NPM2’s second epoch.

### 4.3. Positional Plate Masks

Because the NPM plate model cannot be a perfect representation of the Lick plates, the position residuals will partly reflect whatever unmodeled (e.g., higher-order) positional effects are actually present on the plates. We can check for, and largely correct, these effects by the method of “stacking” the  $347 \times 3$  sets of residuals  $R_X, R_Y$  to make “plate masks.” We stress the importance of doing this separately for the B1, B2, and Y2 plates.

Figures 2, 3, and 4 are the positional plate masks for the B1, B2, and Y2 plates, respectively. We divide the plate into  $14 \times 14 = 196$   $X, Y$  bins, because the faint half of the

Tycho-2 stars were selected in such bins to enforce a uniform distribution of reference stars. Each vector is centered at the mean  $X, Y$  position for the bin, and typically represents the mean residuals  $\langle R_X \rangle, \langle R_Y \rangle$  of  $\langle N_{bin} \rangle \simeq 600$  stars. Several features of the NPM2 plate masks are worth discussing in detail:

1. All three masks (B1, B2, Y2) reveal small ( $\text{RMS} \sim 0.7 \mu\text{m} \simeq 40 \text{ mas}$ ) but highly significant ( $4\sigma$  for B1 and B2;  $6\sigma$  for Y2) systematic patterns that could not have been modeled by cubic terms.
2. The blue plate patterns for the two epochs (Figures 2 and 3) are remarkably similar, a testament to the long-term stability of the Lick astrograph, which is vital to the determination of accurate proper motions. Figure 5 shows the B1 – B2 pattern differences; the RMS vector difference is  $0.4 \mu\text{m} \simeq 20 \text{ mas}$ . (See Section 5 for a comparison with the plate mask from the NPM2 proper motion reductions.)
3. The yellow plate pattern (Figure 4) is quite different from the blue, even though the B2 and Y2 plates for each field were exposed simultaneously. This suggests that the plate patterns reflect optical characteristics of the astrograph’s two lenses, rather than observational effects.
4. The NPM position masks are rather different from the SPM astrograph’s position mask (Figure 4b of Girard et al. 2004), which clearly reveals fifth-order radial distortion effects not seen on the NPM plates.
5. The NPM Y2 plate pattern (Figure 4) is radically different from Figure 9 of Zacharias et al. (2004), which illustrates the “field distortion pattern” (FDP) of NPM Y2 plates vs. Tycho-2, as found in plate reductions for the (unpublished) USNO “Yellow Sky 3” (YS3) catalog. Apparently, that FDP is an artifact of the YS3 reductions.

After we use the plate masks to correct the  $X, Y$  positions on each plate (B1, B2, Y2), any remaining field-dependent errors are reduced to the noise level set by  $\sigma_{pos} / \sqrt{\langle N_{bin} \rangle}$ , which amounts to  $(0.14, 0.12, 0.07) \mu\text{m}$ , or  $(7.7, 6.5, 3.8) \text{ mas}$ , respectively.

#### 4.4. Combined Positions

For each NPM2 field, the final stage in the positional reductions applies the plate constants and the plate-mask corrections to the  $X, Y$  measures, transforms  $X, Y$  to  $\alpha, \delta$ , averages the three positions (B1, B2, Y2) for each star, and checks for discordances.

On each plate, all multiple measures for a given star are averaged. Then, for each star, the 14 positional plate constants (Eqs. 2a and 2b) are applied to transform  $X_M, Y_M$  into the system of the standard coordinates  $X_S = X_M + \Delta X$ ,  $Y_S = Y_M + \Delta Y$ . Next, the appropriate plate-mask correction (B1, B2, or Y2) is applied by adding the mean residuals

$$X_C = X_S + \langle R_X \rangle = X_S + \langle X_T - X_S \rangle \quad (4a)$$

and

$$Y_C = Y_S + \langle R_Y \rangle = Y_S + \langle Y_T - Y_S \rangle \quad (4b)$$

where  $\langle R_X \rangle$  and  $\langle R_Y \rangle$  are interpolated in the  $14 \times 14$   $X, Y$  grid. The mask-corrected standard coordinates  $X_C, Y_C$ , now in the Tycho-2 system, are then transformed into J2000  $\alpha, \delta$ .

The result of the plate reductions is three (two if there is no Y2 measure) separate positions for each star, each at the plate epoch. These are averaged with equal weight, as was done in NPM1. To check for positional discrepancies, we apply each star’s NPM2 proper motion (as determined in Section 5) to bring each position (B1, B2, Y2) from its plate epoch to the mean epoch. The difference between each position and the mean position is calculated. Any star having a residual larger than  $0''.5$  ( $\sim 9 \mu\text{m}$ ) in either coordinate is identified with an error code in the “field catalog” for that field. Any star with a residual larger than  $3''.0$  ( $\sim 54 \mu\text{m}$ ) is rejected. (The rejection rate at this stage is only  $\sim 0.1\%$ .)

The internal errors of the NPM2 mean positions, *at the mean epoch of observation*,  $\sim 1968$ , average  $\sim 80$  mas (RMS) in each coordinate. These results represent a factor-of-two improvement over the precision obtained in NPM1 using a simple quadratic plate model and ACRS reference stars. As noted in (Section 4.3, field-dependent systematic errors of the NPM2 positions are well below 10 mas. This is nearly an order of magnitude better than NPM1, thanks to the Tycho-2-based reductions and the plate-mask corrections.

#### 4.5. Magnitude-Dependent Effects

From our experience with NPM1, we expect that magnitude-dependent effects, on the order of  $1\text{--}2 \mu\text{m}$  in size, may be present in the NPM2 positions. Two questions need to be considered. First, are there “magnitude equations” due to the lack of magnitude terms in the NPM2 plate model (Section 3.2)? Second, how well does the bridge reduction (Section 4.1) put the bright and faint NPM2 stars on the same system?

Effects that are very small in the context of the individual plate reductions, with several

hundred stars per plate, can be detected by comparison of NPM2 with other large positional catalogs, such as Tycho-2 or the new UCAC2 Catalog (Zacharias et al. 2003, 2004).

For bright stars ( $B < 13$ ), we used some 370,000 residuals (Tycho-2 – NPM2) from the B1, B2, and Y2 plate solutions. These were examined versus B magnitude and  $B - V$  color. Small non-linear magnitude effects are seen, with slopes up to  $1 \mu\text{m mag}^{-1}$  ( $55 \text{ mas mag}^{-1}$ ) in  $X$ , and  $0.5 \mu\text{m mag}^{-1}$  ( $30 \text{ mas mag}^{-1}$ ) in  $Y$ . These results are very similar to those previously found by N. Zacharias (2003, private communication), who compared the NPM2 Catalog positions with the UCAC2 Catalog. In addition, the Tycho-2 – NPM2 comparison indicates that these effects may also vary with  $B - V$ , declination, and plate epoch (B1 vs. B2) or plate color (B vs. Y). For NPM2 faint stars ( $13 < m_R < 16$ ; roughly  $14 < B < 17$ ), Zacharias found linear magnitude effects up to  $40 \text{ mas mag}^{-1}$  ( $0.7 \mu\text{m mag}^{-1}$ ) in size.

We have chosen not to correct the NPM2 positions for these magnitude-dependent effects, which are small in the context of NPM2’s positional precision (80 mas near 1968, 200 mas at 2000), and problematical to calibrate in terms of all the observational variables. Users are reminded that NPM is principally a proper motion program. To the extent that these positional effects may vary between epochs, they would affect the NPM2 proper motions, so we do apply magnitude-dependent proper motion corrections (Section 5.4).

The NPM2 – UCAC2 comparison (Zacharias 2003) also verifies that the NPM2 bridge reductions accurately put our bright stars (measured as I(gr) and II(0) images) and faint stars (measured as I(0) images) onto the same positional system. In both right ascension and declination, stars with  $m_R \sim 11$  ( $B \sim 12$ ) and  $m_R \sim 15$  ( $B \sim 16$ ) systematically agree in position to within 10 to 20 mas (0.2 to 0.4  $\mu\text{m}$ ).

## 5. Proper Motions

Absolute proper motions<sup>5</sup> ( $\mu_\alpha$ ,  $\mu_\delta$ ) in each of the 347 NPM2 fields were determined in three steps. First, we perform a differential plate-constant reduction of the B1, B2 plate pair, to obtain relative proper motions. (As in NPM1, the yellow plate Y2 is not used for proper

---

<sup>5</sup>In the NPM program we follow the usual convention of focal-plane astrometry, defining  $\mu_\alpha = \mu \sin \theta$  and  $\mu_\delta = \mu \cos \theta$ , where  $\mu$  is the total proper motion, and  $\theta$  is its position angle in local celestial coordinates (north =  $0^\circ$ , east =  $90^\circ$ ). Thus, both proper motion components are expressed in “great circle measure”, in the same units, ready to use for stellar kinematics. By comparison, positional astronomy usually defines  $\mu_\alpha = d\alpha/dt$ , in terms of an angle subtended at the Pole, which is the form needed to update stellar positions. In Hipparcos’ notation (ESA 1997, Vol. 1, Sec. 1.2.5),  $\mu_{\alpha*} = (d\alpha/dt) \cos \delta$ , which is equivalent to NPM’s  $\mu_\alpha$ .



motions, because there is no Y1 plate for differential reductions.) Second, we apply a plate-mask correction for  $(X, Y)$ -dependent systematics. Third, we correct magnitude-dependent systematic errors and reduce the relative proper motions to absolute. This Section will describe these steps, and assess the accuracy of the NPM2 absolute proper motions.

### 5.1. Plate Constant Reductions

As in NPM1, we determine relative proper motions by a differential plate-constant reduction of the blue plates at the two epochs. We use about 400 faint anonymous stars (“FAS”; Section 2.3) per field, mostly in the range  $15 < B < 17$ , as astrometric reference stars. As discussed in Section 3.2, we use the same plate model (Table 2) as in the positional reductions. The B1 plate coordinates  $X_1, Y_1$  are adjusted to the B2 coordinates  $X_2, Y_2$  in a least-squares solution with the equations of condition

$$\Delta X = X_2 - X_1 = \sum_{i=1}^{14} c_i T_{i,X} \quad (5a)$$

and

$$\Delta Y = Y_2 - Y_1 = \sum_{i=1}^{14} c_i T_{i,Y} \quad (5b)$$

As before,  $c_i$  are the 14 plate constants. The terms  $T_{i,X}, T_{i,Y}$  are evaluated using  $X_1, Y_1$ . All equations are weighted equally, because most of the variance is “cosmic”, i.e. the residuals

$$R_X = X_2 - (X_1 + \Delta X) \quad \text{and} \quad R_Y = Y_2 - (Y_1 + \Delta Y) \quad (6)$$

are largely due to the stellar proper motions. Because the distribution of proper motions in a small area of the sky (Trumpler & Weaver 1953, Sec. 3.52) generally has a sharp core and asymmetric wings, severe trimming of large residuals is necessary. Any star with a vector residual (proper motion) larger than  $20 \mu\text{m}$  (1.1 arcsec) in the first iteration is rejected. Subsequent iterations reject  $3\sigma$  residuals. After convergence, the average number of FAS remaining is about 350. Finally, any FAS with a proper motion larger than  $30 \mu\text{m}$  is flagged for rejection from the NPM2 Catalog. Tests showed that such large FAS motions are occasional spurious results (average 2 per field) of the automated FAS selection process.

Over all 347 NPM2 fields, the RMS unit weight errors of the proper motion plate constant solutions are  $\sigma_{pm} = 4.0 \mu\text{m}$  (220 mas). This corresponds to a proper motion dispersion of  $8 \text{ mas yr}^{-1}$  at the average epoch difference  $\langle \Delta T \rangle = 28 \text{ yr}$ . It is important to note

that  $\sigma_{pm}$  is *not* an error estimate for the NPM2 proper motions, whose PMM measurement precision is  $\sim 2 \mu\text{m} \times \sqrt{2} = 2.8 \mu\text{m}$  (160 mas), corresponding to  $5.6 \text{ mas yr}^{-1}$ ; and whose external accuracy  $\sigma_\mu$  will be evaluated in Sections 5.5 and 7.2.

## 5.2. Proper Motion Plate Mask

Like the position residuals (Section 4.3), the proper motion residuals  $R_X, R_Y$  will partly reflect whatever systematic effects are present on the plates but not in the model. Again, we can check and correct these effects by stacking the  $X, Y$  proper motion residuals to make the mask shown in Figure 6. Here we divide the plate into  $20 \times 20 = 400$   $X, Y$  bins, because the FAS were selected in such bins to enforce a uniform distribution on the plate. Each vector represents the mean residuals  $\langle R_X \rangle, \langle R_Y \rangle$  of an average of 300 stars. The B2 – B1 proper motion mask shows small (RMS  $\sim 0.4 \mu\text{m} \simeq 20 \text{ mas}$ ), complex systematic patterns that are marginally significant ( $1\text{--}2\sigma$ ) for the individual bins, whose precision is limited to  $\sigma_{pm} / \sqrt{300} \simeq 0.2 \mu\text{m}$ . To reduce the scatter, Figure 6 shows a  $3 \times 3$  smoothing of the mean residuals. We use this mask to correct the proper motions of all stars in each NPM2 field.

The plate mask from the NPM2 differential proper motion reductions must reflect changes in the positional patterns of the Lick astrograph’s blue lens between the two epochs, so Figure 6 should resemble the B1 – B2 positional difference<sup>6</sup> pattern in Figure 5. Indeed, comparison of the two masks shows strong similarities in the size and configuration of the patterns, especially near the plate corners and edges where the effects are the largest. The similarity is particularly remarkable because of the totally different sets of stars and methods of reduction the two masks represent. The proper motion reductions use the long-exposure I(0) images of faint stars ( $15 < B < 17$ ) and a differential reduction. The position reductions use the short-exposure II(0) and long-exposure I(gr) images, and an absolute reduction of each plate. These results give confidence that our astrometric plate model is sound and has been successfully applied to the wide range of magnitudes of the stars in NPM2.

## 5.3. Relative Proper Motions

After the FAS plate-constant reductions for a field are done, we calculate the relative proper-motions for all stars, as follows. First, multiple measures for a given star are averaged.

---

<sup>6</sup>The sign of the differences is reversed here because Eq. 2 defines the position residuals as “catalog minus measured.”

Then, for each star, the 14 plate constants (Eqs. 5a and 5b) are applied to transform its measured B1 plate coordinates  $X_1, Y_1$  into the  $X_2, Y_2$  system of the B2 plate, i.e.

$$X_{12} = X_1 + \Delta X \quad \text{and} \quad Y_{12} = Y_1 + \Delta Y. \quad (7)$$

The differences (in the sense B2 – B1) are the raw proper motion displacements

$$D_X = X_2 - X_{12} \quad \text{and} \quad D_Y = Y_2 - Y_{12} \quad (8)$$

to which the mask correction is applied by subtracting the faint reference stars’ mean residuals, so that the corrected proper motion displacements  $P_X, P_Y$  are

$$P_X = D_X - \langle R_X \rangle \quad \text{and} \quad P_Y = D_Y - \langle R_Y \rangle \quad (9)$$

where  $\langle R_X \rangle$  and  $\langle R_Y \rangle$  are interpolated in the  $20 \times 20$   $X, Y$  grid. Next, each star’s relative proper motion components are

$$\mu_X = S_B \times P_X / \Delta T \quad \text{and} \quad \mu_Y = S_B \times P_Y / \Delta T \quad (10)$$

where  $\Delta T$  is the epoch difference (B2 – B1) for that NPM field, and  $S_B = 55.142$  arc-sec mm<sup>−1</sup> (or mas  $\mu\text{m}^{-1}$ ) is the nominal scale of the astrograph’s blue lens.

Finally, we transform the relative proper motion from plate coordinates  $\mu_X, \mu_Y$  into the equatorial components  $\mu_\alpha, \mu_\delta$ . On the  $6^\circ \times 6^\circ$  NPM plates, this is approximately the simple rotation used in NPM1 (Klemola et al. 1971, Fig. 4) to orient  $\mu_\delta$  toward the North Celestial Pole. However, on the gnomonic plate projection,  $\mu_\alpha$  and  $\mu_\delta$  are not strictly orthogonal, and the scale varies slightly over the plate. For NPM2 we use an exact geometric transformation, based on Tissot’s indicatrix (the “ellipse of distortion”), well-known in cartography (Maling 1992; Snyder 1997; Canters 2002) but not in astrometry.

#### 5.4. Corrections to Absolute

Relative proper motions are not useful until they are corrected to an absolute zero point by adding the actual mean motions of the reference stars, determined by other means. NPM1 corrected its proper motions to an absolute system, defined in each field by the mean motion of faint ( $16 < B < 18$ ) galaxies relative to the FAS reference frame. The accuracy of these corrections averaged 2 mas yr<sup>−1</sup> (RMS, per field). Magnitude-dependent corrections were not used, but tests showed that for  $B > 12$ , the bright and faint stars are on the same system, to within 1–2 mas yr<sup>−1</sup>. For the brightest NPM1 stars ( $8 < B < 12$ ), magnitude-dependent systematic errors (“magnitude equations”; Platais et al. 1998b) on the order of 1 mas yr<sup>−1</sup> mag<sup>−1</sup> in  $\mu_\alpha$  and  $\mu_\delta$  were found by comparing NPM1 with Hipparcos.

NPM2 has no reference galaxies, so a different method must be used. For NPM2, we correct the relative proper motions to the system of the Tycho-2 Catalogue, as explained below. In principle this procedure is equivalent to a correction to absolute proper motion, because the Tycho-2 proper motions (Høg et al. 2000a) are on the ICRS/Hipparcos proper motion frame (Kovalevsky et al. 1997), which was linked (rotated) to the inertial extragalactic reference frame defined by NPM1, SPM, and other absolute proper motions (Platais et al. 1998b). In practice, the accuracy of this equivalence fully satisfies the needs of NPM2 (see Section 5.5).

A great advantage of correcting NPM2 to Tycho-2 is that we can calibrate and correct the NPM2 bright stars’ magnitude equations in each coordinate as an integral part of the process. We use Tycho-2, rather than Hipparcos as we had originally intended (Hanson 1997), because we now have some 350 Tycho-2 stars per field in the needed magnitude range ( $9 < B < 13$ ). This is ten times the number of Hipparcos stars useful for this purpose. Tests showed the precision of the NPM2–Tycho-2 corrections in an average field is  $\sim 0.5 \text{ mas yr}^{-1}$ , a factor of three better than we could have achieved using Hipparcos stars.

The magnitude equations vary substantially from field to field, so we calibrate and correct them separately in each NPM2 field. To do this, we used  $\Delta\mu_\alpha$  and  $\Delta\mu_\delta$  (Tycho-2 absolute minus NPM2 relative), with a least-squares solution in each coordinate, with the equations of condition

$$\Delta\mu_\alpha = a_0 + a_1 (B - 12) + a_2 (B - 12)^2 \quad (11a)$$

and

$$\Delta\mu_\delta = b_0 + b_1 (B - 12) + b_2 (B - 12)^2 \quad (11b)$$

The  $B$  magnitudes are the NPM2 photometry, discussed in Section 6. The comparison is restricted to the magnitude range  $9 < B < 13$ . Solutions in each coordinate were iterated until no  $3\sigma$  residuals remained. After convergence, the numbers of stars used averaged 350 in each coordinate, and the unit weight errors averaged 6.9 and 7.3  $\text{mas yr}^{-1}$  in  $\Delta\mu_\alpha$  and  $\Delta\mu_\delta$ , respectively. The linear magnitude terms ( $a_1, b_1$ ) averaged  $(+1.3, +2.3) \text{ mas yr}^{-1} \text{ mag}^{-1}$ , and typically were  $3\text{--}4\sigma$  significant in each field. The quadratic magnitude terms ( $a_2, b_2$ ) averaged  $(-0.4, -0.5) \text{ mas yr}^{-1} \text{ mag}^{-2}$ , and typically were  $2\sigma$  significant in each field.

Adding the  $\Delta\mu_\alpha, \Delta\mu_\delta$  corrections (Eqs. 11a,b) to each bright star’s relative proper motion is equivalent to correcting the linear ( $a_1, b_1$ ) and quadratic ( $a_2, b_2$ ) magnitude equations to a fiducial magnitude,  $B = 12$ , and then applying zero-point corrections ( $a_0, b_0$ ) from relative to absolute proper motion.

The fiducial magnitude  $B = 12$  is where the NPM photography optimized the I(gr) and II(0) images. In our view, the magnitude equations reflect the circumstance that on the NPM blue plates, the overexposed I(0) image progressively encroaches on the grating and short-exposure images as  $B \rightarrow 8$ , the limit of useful measurement (du Mont 1978). For this reason, the magnitude-dependent part of the corrections determined here applies only to bright stars, not to the faint ( $B \gtrsim 14$ ) stars whose isolated I(0) images were used.

The zero-point corrections ( $a_0, b_0$ ) defined at the fiducial magnitude  $B = 12$ , and derived from bright stars, apply to the faint stars as well, because the bridge reductions (Section 4.1) put all stars on the I(0) system. In this view,  $a_0, b_0$  simply reflect the mean motions of the faint ( $B \sim 16$ ) reference stars on the Tycho-2 system.

So, distinguishing “bright” and “faint” stars according to what image systems were measured, the corrections for bright stars are

$$\mu_\alpha(abs) = \mu_\alpha(rel) + \Delta\mu_\alpha \quad \text{and} \quad \mu_\delta(abs) = \mu_\delta(rel) + \Delta\mu_\delta \quad (12)$$

and for faint stars, we have

$$\mu_\alpha(abs) = \mu_\alpha(rel) + a_0 \quad \text{and} \quad \mu_\delta(abs) = \mu_\delta(rel) + b_0. \quad (13)$$

These corrections put all the stars onto an absolute system, as defined by the Tycho-2 stars. The precision of the  $\Delta\mu$  corrections in an NPM2 field is about  $0.5 \text{ mas yr}^{-1}$ , the RMS size of the errors of  $a_0$  and  $b_0$  from Eqs. 11.

### 5.5. Accuracy of the Absolute Proper Motions

The internal (measurement) errors of the NPM2 proper motions are  $\sim 5.6 \text{ mas yr}^{-1}$  (Section 5.1). Comparison of multiple measures from field overlaps (Section 7.2) estimates the RMS external accuracy of an individual proper motion to be  $5.9 \text{ mas yr}^{-1}$ .

Many of the intended uses of the NPM2 proper motions in stellar kinematics and galactic astronomy essentially involve averaging the motions of large numbers of stars. In this context, the following question arises:

Without directly linking NPM2 to Hipparcos, how closely can we say that NPM2 is on the Hipparcos (ICRS) proper motion system? Tycho-2 is nominally on the Hipparcos system. From direct comparisons, using all 119,740 stars in common to the two catalogs, Høg et al. (2000a) concluded that the systematic errors of the Tycho-2 proper motions are  $\lesssim 0.5 \text{ mas yr}^{-1}$  on angular scales of  $6^\circ$  or more (the size of the Lick plates, coincidentally), making the conservative assumption that Hipparcos’ systematic errors are negligible. Høg

et al. (2000a) could not rule out that larger differences might exist on smaller angular scales, such as the  $2^\circ \times 2^\circ$  size of the Astrographic Catalogue plates. Presumably this is because of small-number statistics; the number of stars to compare averages just  $3 \text{ deg}^{-2}$ . In any event, for NPM2 the relevant angular scale is that of the Lick plates.

As a test for NPM2, we compared the Tycho-2 and Hipparcos proper motions, field by field, in the 347 NPM2 fields. This was done twice: first, for all stars in common and second, in the limited magnitude range  $9 < B < 13$  used by NPM2. Outliers with  $|\Delta\mu| > 10 \text{ mas yr}^{-1}$  in either coordinate were trimmed in order to restrict the comparisons to the most accurate data.

In the all-star comparison (30,517 stars; average 88 per field), the RMS values of  $\langle\Delta\mu_\alpha\rangle$  and  $\langle\Delta\mu_\delta\rangle$  were 0.18 and 0.17  $\text{mas yr}^{-1}$ , only  $\sim 3\%$  larger than the internal ( $\sigma/\sqrt{N}$ ) errors. Only one of 347 NPM2 fields had  $\langle\Delta\mu\rangle$  larger than 0.5  $\text{mas yr}^{-1}$  in either coordinate. The Høg et al. (2000a) limit is quite conservative, being in effect a  $3\sigma$  limit.

In the faint-star comparison (14,323 stars; average 41 per field), the RMS values of  $\langle\Delta\mu\rangle$  were substantially larger, 0.28 and 0.30  $\text{mas yr}^{-1}$ . This reflects the lower precision of the  $\Delta\mu$  values for stars this faint (Høg et al. 2000a, Table 1). Again, the  $\langle\Delta\mu\rangle$  values were about the size of the internal errors. None of 347 NPM2 fields had  $\langle\Delta\mu\rangle$  larger than 1.0  $\text{mas yr}^{-1}$  in either coordinate.

The main result of these proper motion comparisons is that, on the  $6^\circ \times 6^\circ$  angular scale of the NPM fields, any differences between the Tycho-2 and Hipparcos proper motion systems are in effect too small to measure. Formally, the external/internal error ratio (1.03) in the all-star comparison suggests that systematics on the order of 0.05  $\text{mas yr}^{-1}$  (RMS) may be present, but this result is far from exact.

For NPM2, the RMS dispersion 0.3  $\text{mas yr}^{-1}$  from the faint-star comparisons is the relevant limit on how closely our reduction of the NPM2 proper motions to Tycho-2 is the equivalent of reducing them to the Hipparcos system. In practice, for a given NPM2 field, this adds quadratically to the 0.5  $\text{mas yr}^{-1}$  error of the NPM-Tycho corrections. So, the NPM2 proper motions are on the Hipparcos (ICRS) system to an accuracy of 0.6  $\text{mas yr}^{-1}$ .

## 6. Photometry

In each NPM2 field, the PMM instrumental magnitudes  $m_b$  and  $m_y$  are reduced into  $B$  magnitudes and  $B - V$  colors, with multiple measures for each star combined into a single magnitude and color. Our experience with NPM1 and our tests for NPM2 (see Section 7.2)

show that the RMS errors of the NPM photographic photometry are about 0.2 mag in  $B$  and the same in  $B - V$ . Color errors for very faint, red, or blue stars can be substantially larger. We caution readers of this paper, and users of the NPM Catalogs, that the Lick astrograph plates are not suitable for more accurate photometry. The NPM1 and NPM2 magnitudes and colors are accurate enough for statistical discussion of the proper motions, which is their intended purpose.

Rather than describing the NPM2 photometric reductions in detail, we will give a broad outline, emphasizing several systematic improvements over the NPM1 procedures described in Paper I:

1. On each plate (B1, B2, Y2), we reduce the bright stars' ( $B \lesssim 14$ ) long-exposure grating image photometry into the short-exposure II(0) system. In each field, we reduce every star's B1 photometry into the system of the B2 plate. For further reductions,  $m_b$  is taken as the mean of the B1 and B2 measures (both in the B2 system). No photometric standards are needed for these differential reductions.<sup>7</sup> Plate-constant models use six terms: zero point,  $m_b$  or  $m_y$ ,  $X$ ,  $Y$ ,  $X^2$ , and  $Y^2$ .
2. We use the Tycho-2 photometry ( $B_T, V_T$ , reduced to Johnson  $B, V$  using Eqs. 1.3.20 of ESA 1997), as supplementary standards. This gives an order-of-magnitude increase over the number of primary standard stars (ICSS stars with BV photometry; Table 1) available per field.
3. For faint stars ( $B \gtrsim 14$ ), measured as I(0) images, we derive  $B$  and  $V$  magnitudes after differentially calibrating the  $\sim 4$  mag long–short exposure difference on each plate, effectively extending the Tycho-2 photometric standards 4 mag fainter. A simple plate model (zero point and linear magnitude term) usually suffices for this. Separate solutions are done in each color. Typically, 20 to 30 faint photometric standard stars are used.
4. Plate models transforming  $m_b$  into  $B$ , and  $m_y$  into  $V$  use six terms: zero point,  $m$ ,  $m^2$ , and field terms  $X$ ,  $Y$ , and  $R^2 = X^2 + Y^2$ . Internal errors average 0.25 mag for bright stars, 0.30 mag for faint stars. These values overestimate the true errors (Section 7.2) of the NPM2 photometry, because of the limited accuracy of the photometric standards.

---

<sup>7</sup>For historical accuracy, we note that these “photometric bridge reductions” were actually used in the 1993 NPM1 Catalog reductions, but had not been devised at the time Paper I (Klemola, Jones, & Hanson 1987) was written.

5. For bright stars, the  $B - V$  color is directly calculated from  $B$  and  $V$ . For faint stars,  $B - V$  is also determined from the instrumental color  $m_b - m_y$ , using the statistical method used for NPM1 (Section VIIIe of Paper I); the color adopted for NPM2 is generally the mean of the two methods. For  $\sim 1.5\%$  of NPM2 stars,  $B - V$  is not determined, usually because the yellow plate measure is lacking.
6. For fainter Tycho-2 stars ( $11 \lesssim B \lesssim 14$ ), the precision of the Tycho-2 photometry (see Table 2 of Høg et al. 2000b) is comparable to NPM2. For brighter stars, the Tycho-2 errors are much smaller than NPM2. Consequently, for all Tycho-2 stars in the NPM2 catalog, we adopt the error-weighted mean of the Tycho-2 and NPM2  $B$  magnitudes and  $B - V$  colors.

## 7. Lick NPM2 Catalog

In this Section we outline the compilation and final content of the Lick NPM2 Catalog, determine the external errors of the NPM2 positions, proper motions, and photometry, and compare these to the results achieved for NPM1. We also describe two important supplements to the NPM2 Catalog: the NPM2 Cross-Identifications list and Klemola’s ICSS Star Identification Catalog.

### 7.1. Catalog Compilation

The NPM2 data reductions yielded 347 partially overlapping “field catalogs”, with a raw total of 288,615 stars (average  $\sim 830$  per field). Following the procedures used in the production of the NPM1 Catalog (Hanson 1997), the NPM2 Catalog was compiled by merging and combining data from the field catalogs. First, each position was updated from its mean plate epoch ( $\sim 1968$ ) to the common catalog epoch 2000, by applying the NPM2 proper motions. Then the stars were sorted into a one-degree zone-catalog format, with multiple measures (up to four per star) from the field overlaps ( $\sim 1^\circ$ ) averaged to give one entry per star, as in NPM1. No block adjustments were done, because of the need to preserve the statistical independence of each field, which is important for galactic and astrometric applications of the NPM data. The field overlaps were used to estimate the external errors of the NPM2 positions, proper motions, magnitudes, and colors, as well as to reject the small fraction ( $< 0.1\%$ ) of erroneous measurements not previously detected in the plate reductions, and to “flag” stars with discordant astrometry or photometry.

The completed Lick NPM2 Catalog (Hanson et al. 2003), contains 232,062 stars, a



reduction of 20% from the raw total of the 347 field catalogs. The catalog, in 108 one-degree declination zone files from  $+83^\circ$  to  $-23^\circ$ , was released on our WWW site<sup>8</sup> in May 2003, along with extensive documentation, including error estimates and file format details, in an accompanying “ReadMe” file. The NPM2 Catalog is also available in the form of one 26 Mb file (compressed to 6.4 Mb) concatenating the 108 zones. This version was also deposited at the CDS Strasbourg data center (catalog number I/283A), where it is available by ftp and accessible by VizieR query.

Table 3 illustrates the format and content of the NPM2 Catalog. Following the convention of the NPM1 Catalog, each star is indexed by an NPM2 “name” (e.g. +83.0001) reflecting the declination zone and a running number in J2000 right ascension order within the zone. Each star’s entry includes the absolute proper motion ( $\mu_\alpha, \mu_\delta$ ) and  $B$  magnitude. For 98.5% of the stars the  $B - V$  color is also given. Other data given for each star are: the original mean epoch, a stellar class code, the number of NPM fields ( $N_F$ ) on which the star was measured, and discrepancy flags for position, proper motion, and photometry.

The NPM2 Catalog also lists identifications for 90,690 Tycho-2 stars, 20,426 stars from the ACRS catalog, and 8,437 Hipparcos stars. These categories overlap greatly. The positional catalog stars total 91,648; nearly all have  $B < 14$ . Non-catalog NPM2 stars are mostly faint ( $B > 14$ ); 122,806 are anonymous stars chosen for astrometric and galactic studies. The NPM2 Catalog contains 34,868 “special stars” from Klemola’s ICSS; about half of these have  $B < 13$ , and overlap substantially with the catalog stars. Identifications for the NPM2 “special stars” are discussed in Section 7.3.

## 7.2. External Errors

Because the NPM fields (Figure 1) overlap by at least  $1^\circ$  in each direction, the NPM2 catalog has 45,143 stars with multiple measures in overlapping NPM2 fields (37,854 stars have  $N_F = 2$ ; 4,201 have  $N_F = 3$ ; and 3,088 have  $N_F = 4$ ). Another 2,642 NPM2 stars overlap with NPM1 at the edges of the Milky Way. Because the NPM fields were measured and reduced separately, the multiple measures from overlapping fields are statistically independent, so that the RMS dispersion of the 2, 3 or 4 multiple measures about the mean value used in the NPM2 Catalog can be used to estimate the external errors of the NPM2 positions, proper motions, magnitudes, and colors.

Table 4 compares the NPM2 external errors with the internal error (precision) estimates

---

<sup>8</sup><http://www.ucolick.org/~npm/NPM2>

derived in Sections 4, 5, and 6. We also compare the NPM2 errors with the NPM1 Catalog errors given by Hanson (1997).

For the NPM2 positions, the internal errors at the mean plate epoch ( $\sim 1968$ ) are calculated from the RMS residuals for the three sets (B1, B2, Y2) of plate reductions (Section 4.2). The external errors of the NPM2 positions were derived twice. At the NPM2 Catalog epoch 2000, the positional errors are the quadratic sum (see Eq. 1) of the pure positional errors at the mean plate epoch and the proper motion error accumulated from the mean epoch to 2000. To evaluate the pure positional errors, we did a second overlap comparison using NPM2 positions computed for the epoch 1968. (The same procedure was used for NPM1.) The external errors at epoch 1968 are only  $\sim 10\%$  larger than the internal error estimates, and nearly a factor of two better than NPM1.

For the NPM2 proper motions, internal errors cannot be obtained from the plate solutions, because the residuals largely represent stellar motions, not measurement errors. Table 4 lists the precision of an individual proper motion measurement as estimated in Section 5.1, assuming  $2\mu\text{m}$  PMM measurement errors at each epoch and a 28 yr mean epoch difference  $\langle B2-B1 \rangle$ . The external errors from the field overlap comparisons are  $\sim 10\%$  larger. The NPM2 proper motion errors are  $\sim 10\text{--}20\%$  larger than NPM1; this may reflect a slightly higher precision for the Lick AME measurements used in NPM1.

The precision of the NPM2 absolute zero point errors is estimated by the RMS dispersion of the mean proper motion differences  $\langle \text{Tycho-2-NPM2} \rangle$  for 347 NPM2 fields (Section 5.4). The external error listed in Table 4 is the value derived in Section 5.5 for the accuracy to which each NPM2 field has been put onto the ICRS proper motion system. These values are 3–4 times better than the zero point error in a typical NPM1 field, where  $\sim 80$  galaxies were used to correct the proper motions to absolute.

For the NPM2 photometry, the RMS residuals from NPM2 plate reductions somewhat overestimate the internal errors because of the limited accuracy of the photometric standards. In Table 4 the internal error given for the NPM2  $B$  magnitudes is the lower end of the range found in Section 6. From our experience in NPM1 and NPM2, we adopt the same value for the  $B - V$  colors. To obtain valid external errors for  $B$  and  $B - V$ , these were evaluated from field overlap comparisons using a version of the NPM2 Catalog that did *not* average in any Tycho-2 photometry. The photometric errors derived here apply to (generally faint) non-Tycho-2 stars in the NPM2 Catalog. Overall, the NPM2 PMM photometry is roughly as accurate as NPM1’s AME photometry.

Overlap comparisons were also done using 2,642 stars in common between the NPM1 and NPM2 Catalogs. Mean and RMS differences were calculated after trimming 5% of the

outliers from each tail of the distribution. Positions were compared at the epoch 1968. The RMS differences were 210 mas in  $\Delta\alpha$  and 230 mas in  $\Delta\delta$ . These are 20–30% larger than expected from the errors listed in Table 4. Positional zero point errors of order 100 mas in the individual NPM1 fields are the likely cause. The RMS proper motion differences were 7.0 mas yr<sup>−1</sup> in  $\Delta\mu_\alpha$  and 8.0 mas yr<sup>−1</sup> in  $\Delta\mu_\delta$ . RMS photometry differences were 0.27 mag in  $B$  and 0.26 mag in  $B - V$  (2,478 stars). The proper motion and photometry differences are consistent with the NPM1 and NPM2 errors in Table 4.

We note that the NPM2 and NPM1–NPM2 field overlap error estimates were all derived using stars within  $\sim 1^\circ$  of the edges of the  $6^\circ \times 6^\circ$  Lick plates, and may overestimate the errors of the majority of stars, which are closer to the plate centers, where the image quality is better. Also, the errors listed in Table 4 pertain to a single measurement on one NPM2 field. The data listed in the NPM2 Catalog for the 45,143 stars with  $N_F > 1$  are means of  $N_F = 2, 3$ , or 4 measures, and their actual errors should be  $N_F^{-0.5}$  times smaller, in the absence of systematic errors. To be conservative, we chose to cite the single-measurement errors in Table 4 to represent the overall accuracy of the NPM2 data. Finally, we note that the astrometric errors for stars brighter ( $B < 10$ ) or fainter ( $B > 17$ ) than the optimal range of measurement on the Lick plates tend to be somewhat larger than the values listed in Table 4.

### 7.3. NPM2 Cross-Identifications

To assist users of the NPM2 Catalog, we have compiled a supplementary catalog, the NPM2 Cross-Identifications and Appendices (NPM2 Cross-IDs; Klemola et al. 2004), much as we did for NPM1 (Klemola, Hanson, & Jones 1994). This catalog was released on our WWW site in March 2004, and will be available at the CDS data center (catalog number I/293). The NPM2 Cross-IDs file, with 46,887 entries, lists star names, stellar type classifications, and publication references for the 34,868 NPM2 “special stars.” (ICSS stars have multiple identities when chosen under more than one category of interest.) Many of these identifications from the literature had been uncertain or ambiguous, and were verified by Klemola at the Lick Survey Machine, usually from finding charts, variability, or proper motion. After the NPM2 positions were available, Klemola re-confirmed many of these identifications using the CDS SIMBAD and NASA SkyView databases, as well as recent catalogs listing improved positions for variable stars, carbon stars, and other categories. Based on this work, the NPM2 Cross-IDs file gives a reliability code for each stellar identification.

Four Appendices to the NPM2 Catalog detail the 570 literature references and list the 164 stellar (occasionally, non-stellar) classes from which the NPM2 “special stars” were

selected. A fifth Appendix provides 1,847 footnotes to the NPM2 Catalog. A “ReadMe” file briefly summarizes the NPM2 Cross-IDs and provides file formats. Another text file gives detailed documentation on the compilation and content of the NPM2 Cross-IDs, and discusses the Lick ICSS and its relation to the NPM Catalogs.

The NPM2 Cross-Identifications will facilitate many practical uses of the NPM2 Catalog, allowing users to select “special stars” by category (e.g. RR Lyrae variables, white dwarfs, faint blue stars, etc.) or from specific catalogs or literature sources, as well as to identify individual stars of interest. We are using the NPM1 and NPM2 Cross-Identifications files to produce combined NPM1 + NPM2 “mini-catalogs” for use in galactic astronomy. We intend to post these on our WWW site. Major categories of interest include 6000 OB stars, 5100 faint blue stars/objects, 4900 red giants, 3900 emission-line stars, 3500 high-proper-motion stars, 2100 RR Lyrae type variables, 1600 white dwarf stars/candidates, 1100 horizontal branch stars, and 900 carbon stars. Variable stars of all types total 12,500. Halo population stars total about 5000. (These counts are preliminary, and may change when individual categories are studied in detail.)

#### 7.4. ICSS Star Identification Catalog

For numerous reasons, Klemola’s ICSS contains many stars that are not included in the NPM Catalogs. The ICSS has been continually updated for completeness, but it was not practical for NPM1 to include stars from sources published after the plates were measured. Few NPM2 fields were re-surveyed for additional stars. Later additions to the ICSS could now be recovered from the PMM scans, but that is beyond the scope of the Lick program. For both NPM1 and NPM2, many ICSS stars could not be reliably identified at the Survey Machine, chiefly because of poor positions or lack of finding charts. In all, about 46% of the 123,000 ICSS stars in the 347 NPM2 fields were not selected in the plate surveys. For NPM2, another 14% of the ICSS stars were identified at the Survey Machine but were coded for rejection before the PMM star selection stage. Very bright stars ( $B \lesssim 9$ ), or stars too faint ( $B \gtrsim 18$ ) for useful measurement were not generally accepted for NPM2. Variable stars with large amplitude often did not have useful images at both epochs. Many stars had no unblended images to use, due to crowding in the dense low-latitude fields. The loss fraction for “special stars” is much larger than for catalog or anonymous stars, where we had more freedom to reject problematic stars, and choose substitutes, on the PMM scans. Another 4% of the ICSS stars were not selected on both the B1 and B2 PMM scans. These stars cannot be used for NPM2. Finally, 7% of the ICSS stars were rejected at various stages in the NPM2 data reductions, when faint, blended or otherwise unsuitable images caused large residuals.

In all, the 34,868 (of 123,000) ICSS stars in the NPM2 Catalog represent a survival rate less than 30%. The high attrition of “special stars” in NPM2 is an unfortunate consequence of our conservative policy of minimizing spurious results by aggressively rejecting problematic stars.

Although many ICSS stars were “lost” to NPM2, Klemola’s plate surveys contain much information of value to observers and database compilers. Over 30,000 ICSS stars not in NPM2 were positively identified at the Survey Machine, and their  $X, Y$  coordinates were visually measured with  $\sim 20 \mu\text{m}$  precision,  $\sim 1$  arcsec on the NPM plates. This often represents an order-of-magnitude improvement over the previous crude positions. Klemola will compile a “Star Identification Catalog” (SIC) with confirmed identifications and arcsecond-level positions for this subset of the ICSS. The SIC data will be a valuable contribution to stellar databases such as SIMBAD, and will prove useful for identifying stars in existing and future databases, and facilitating further observations for many stars of particular astronomical or astrophysical interest.

## 8. Summary and Discussion

The two NPM Catalogs total 378,360 stars (148,940 in NPM1 plus 232,062 in NPM2, less 2,642 in both due to plate overlaps) from  $8 \lesssim B \lesssim 18$ , covering the northern two-thirds of the sky ( $\delta \gtrsim -23^\circ$ ). NPM2 covers only  $\sim 40\%$  of the sky area of NPM1, but its star density is four times as high. This partly reflects that many classes of stars are strongly concentrated towards the galactic plane. A particular scientific value of NPM2 lies in its low-latitude ( $|b| < \sim 10^\circ$ ) sky coverage. Important tracers of the galactic disk and spiral arms (Cepheids, OB stars) are generally found only at low latitudes. Other classes of stars in the Lick Input Catalog of Special Stars that are chiefly represented at low latitudes are carbon stars, red giants, and many types of variable stars. Even halo population stars such as the RR Lyrae variables are found in large numbers at lower galactic latitudes in the NPM survey, because of their concentration toward the galactic center. Many of the 34,868 NPM2 “special stars” are too distant, and thus too faint, to be represented in significant numbers in the Hipparcos or Tycho Catalogues. The NPM2 Catalog also includes two large, kinematically unbiased, sets of stars useful for studies of galactic structure and kinematics: 91,648 positional catalog stars with  $B \lesssim 14$ ; and 122,806 faint ( $B \gtrsim 14$ ) anonymous stars.

Because the long-term value of the NPM proper motions depends critically on their precision and accuracy, great effort was devoted to testing their quality, with the goal of calibrating and eliminating systematic errors. Repeated tests confirmed the high precision and accuracy of the NPM1 proper motions (Hanson 1987, 1997; Platais et al. 1998b). As

detailed in Table 4, this level of quality has been met or exceeded for NPM2. The RMS errors over the magnitude range  $10 < B < 17$  are 5–6 mas yr<sup>−1</sup> for both catalogs. The absolute zero point of proper motion, determined independently in each NPM field, is accurate to 2 mas yr<sup>−1</sup> for NPM1, and 0.6 mas yr<sup>−1</sup> for NPM2.

The high quality of the NPM proper motions has also been demonstrated in their applications to several problems in galactic structure and astrometry, such as the solar motion and galactic rotation (Hanson 1987), the absolute motions of 14 globular clusters (Cudworth & Hanson 1993), the statistical parallax luminosity calibration of 200 RR Lyrae stars (Layden et al. 1996), and the linking of Hipparcos to the inertial proper motion system (Platais et al. 1998b). In particular, the latter two results confirm that the absolute proper motion zero points for the NPM “bright” ( $B \sim 12$ ) and “faint” ( $B \sim 16$ ) stars are consistent to better than 1 mas yr<sup>−1</sup>.

The NPM2 positions at 1968, near the mean epoch of observation, are twice as precise as NPM1 (RMS error 80 mas for NPM2, 150 mas for NPM1), and their systematic accuracy is ten times better (10 mas for NPM2, 100 mas for NPM1). These improvements are due to the use of a much better plate model, and an order of magnitude more reference stars per field, than NPM1. The NPM2 photographic positions, though not having the high precision of modern positional catalogs, are in fact of comparable or better quality than Tycho-2 for  $V \geq 11.5$  (see Table 2 and Figure 2 of Høg et al. 2000b). Likewise, the RMS errors ( $\sim 0.2$  mag) of the NPM2 photographic photometry, which was chiefly intended for statistical use, equal or surpass Tycho-2 for  $V \geq 12$ .

The publication of the NPM2 Catalog and Cross-IDs in 2003-4 completes the Lick Northern Proper Motion program as it was originally conceived, but it does not mean that our work is concluded. Much can be done to apply the NPM data to important research problems in galactic structure, stellar kinematics, and astrometry. Applications now underway at Lick include: (1) extension of the NPM1 (Hanson 1987) galactic rotation and solar motion study to cover the sky north of  $-23^\circ$  and to determine  $dV/d|Z|$ , the progressive lag behind circular rotation with distance from the galactic plane, due to the changing mix of stellar populations with different scale heights; and (2) use of the NPM1 and NPM2 Cross-IDs, and the method of reduced proper motions, for a comprehensive identification of  $\sim 5,000$  halo population stars in the two catalogs.

Many other uses of the NPM1 and NPM2 data can be foreseen. The two Lick NPM Catalogs uniquely represent a small, but carefully chosen and rigorously reduced, subset of stars in the northern two-thirds of the sky, intended to serve as a database for galactic research needing accurate proper motions for stars selected with little or no kinematic bias, and to supply proper motions for well-identified stars in categories of high astronomical

interest. The PMM scans of all 1,246 NPM fields, containing data for several hundred million stars, are another important product of the NPM program, which can be used to expand the NPM Catalogs, much as the Yale SPM program is doing in the southern sky, or to incorporate data from the Lick plate epochs into modern all-sky proper motion catalogs.

The Northern Proper Motion program represents a half-century of work by three generations of astronomers at Lick Observatory, whose contributions were acknowledged in some detail in Paper I. Once again, we thank W.H. Wright, C.D. Shane, C.A. Wirtanen, S. Vasilevskis, and E.A. Harlan for the foresight, innovation, and dedication that brought the NPM program to the point where we could successfully complete it. We also thank the National Science Foundation for its long-term support of the Lick NPM program. The NPM2 phase was supported by NSF grants AST-9530632 and AST-9988105. We thank the Yale Southern Proper Motion group (W.F. van Altena, I. Platais, and T.M. Girard) for their help in developing software to process the PMM plate scans, and we thank the staff members of the US Naval Observatory Flagstaff Station who scanned nearly 4,000 NPM plates on the PMM. We thank Norbert Zacharias (USNO) for making the NPM2 – UCAC2 positional comparison. We thank Imants Platais for his detailed, thoughtful, and prompt referee’s report. This research has made use of the SIMBAD database, operated at CDS, Strasbourg, France.

## REFERENCES

- Beers, T. C., Chiba, M., Yoshii, Y., Platais, I., Hanson, R. B., Fuchs, B., & Rossi, S. 2000, *AJ*, 119, 2866
- Canter, F. 2002, *Small-Scale Map Projection Design* (London and New York: Taylor and Francis)
- Corbin, T. E., Urban, S. E., & Warren, W. H. Jr. 1991, *Astrographic Catalog Reference Stars* (Washington: U.S. Naval Observatory), CDS Strasbourg Data Center Catalog No. I/171
- Cudworth, K.M. & Hanson, R.B. 1993, *AJ*, 105, 168
- du Mont, B. 1978, *A&A*, 66, 441
- ESA 1997, *The Hipparcos and Tycho Catalogues*, ESA Publication SP-1200 (Noordwijk: ESA), CDS Strasbourg Data Center Catalog No. I/239

- Girard, T. M., Platais, I., Kozhurina-Platais, V., van Altena, W. F., & López, C. E. 1998, *AJ*, 115, 855
- Girard, T. M., Dinescu, D. I., van Altena, W. F., Platais, I., Monet, D. G., & López, C. E. 2004, *AJ*, 127, 3060
- Gliese, W. & Jahreiss, H. 1991, Third Catalogue of Nearby Stars, Preliminary Version (Heidelberg: Astron. Rechen-Institut), CDS Strasbourg Data Center Catalog No. V/70A
- Hanson, R. B. 1987, *AJ*, 94, 409
- Hanson, R. B. 1997, in *ASP Conf. Ser. 127, Proper Motions and Galactic Astronomy*, ed. R. M. Humphreys, (San Francisco: ASP), 23
- Hanson, R. B., Klemola, A. R., Jones, B. F., & Monet, D. G. 2003, Lick Northern Proper Motion Program: NPM2 Catalog, CDS Strasbourg Data Center Catalog No. I/283A <http://www.ucolick.org/~npm/NPM2>
- Høg, E., Fabricius, C., Makarov, V. V., Bastian, U., Schwekendiek, P., Wicenec, A., Urban, S., Corbin, T., & Wycoff, G., 2000a, *A&A*, 357, 367.
- Høg, E., Fabricius, C., Makarov, V. V., Urban, S., Corbin, T., Wycoff, G., Bastian, U., Schwekendiek, P., & Wicenec, A. 2000b, *A&A*, 355, L27. CDS Strasbourg Data Center Catalog No. I/259
- Kholopov, P. N., Samus, N. N., Frolov, M. S., & 12 co-authors 1998, CDS Strasbourg Data Center Catalog No. II/214A
- Klemola, A. R., Hanson, R. B., & Jones, B. F. 1993a, Lick Northern Proper Motion Program: NPM1 Catalog, CDS Strasbourg Data Center Catalog No. I/199
- Klemola, A. R., Hanson, R. B., & Jones, B. F. 1993b, Lick Northern Proper Motion Program: NPM1 Reference Galaxies, CDS Strasbourg Data Center Catalog No. I/200
- Klemola, A. R., Hanson, R. B., & Jones, B. F. 1994, Lick Northern Proper Motion Program: NPM1 Catalog Cross-Identifications and Appendices, CDS Strasbourg Data Center Catalog No. I/214 <http://www.ucolick.org/~npm/NPM1/crossid>
- Klemola, A. R., Hanson, R. B., & Jones, B. F. (1995), in *Galactic and Solar System Optical Astrometry*, ed. L. V. Morrison & G. F. Gilmore (Cambridge: Cambridge University Press), 20



- Klemola, A. R., Hanson, R. B., & Jones, B. F. 2000, Lick Northern Proper Motion Program: NPM1 Catalog (J2000 Version), CDS Strasbourg Data Center Catalog No. I/199A <http://www.ucolick.org/~npm/NPM1>
- Klemola, A. R., Hanson, R. B., Jones, B. F., & Monet, D. G. 2004, Lick Northern Proper Motion Program: NPM2 Catalog Cross-Identifications and Appendices, CDS Strasbourg Data Center Catalog No. I/293 <http://www.ucolick.org/~npm/NPM2/crossid>
- Klemola, A. R., Jones, B. F., & Hanson, R. B. 1987, *AJ*, 94, 501 (Paper I)
- Klemola, A. R., Vasilevskis, S., Shane, C. D., & Wirtanen, C. A. 1971, *Publ. Lick Obs.*, 22, Part II
- König, A., in *Astronomical Techniques*, ed. W. A. Hiltner (Chicago: Univ. of Chicago Press), 461
- Kovalevsky, J., Lindegren, L., & Perryman, M. A. C. 1997, Ch. 18 in Vol. 3 of *The Hipparcos and Tycho Catalogues*, ESA Publication SP-1200 (Noordwijk: ESA), 387
- Layden, A. C., Hanson, R. B., Hawley, S. L., Klemola, A. R., & Hanley, C. J. 1996, *AJ*, 112, 2110
- Luyten, W. J. 1991, *New Luyten Catalogue of Stars With Proper Motions Larger Than Two Tenths of an Arcsecond* (Minneapolis: University of Minnesota), CDS Strasbourg Data Center Catalog No. I/98A (NLTT)
- Maling, D. H. 1992, *Coordinate Systems and Map Projections* (2nd ed.; Oxford: Pergamon Press)
- Monet, D. G., Levine, S. E., Canzian, B., & 25 coauthors 2003, *AJ*, 125, 984
- Platais, I., Girard, T. M., van Altena, W. F., Ma, W. Z., Lindegren, L., Crifo, F., & Jahreiss, H. 1995, *A&A*, 304, 141
- Platais, I., Girard, T. M., Kozhurina-Platais, V., van Altena, W. F., López, C. E., Mendez, R. A., Ma, W.-Z., Yang, T.-G., MacGillivray, H. T., & Yentis, D. J. 1998a, *AJ*, 116, 2556
- Platais, I., Kozhurina-Platais, V., Girard, T. M., van Altena, W. F., López, C. E., Hanson, R. B., Klemola, A. R., Jones, B. F., MacGillivray, H. T., Yentis, D. J., Kovalevsky, J., & Lindegren, L. 1998b, *A&A*, 331, 1119

- Snyder, J. P. 1997, *Flattening the Earth: Two Thousand Years of Map Projections* (Paperback ed.; Chicago: University of Chicago Press)
- Trumpler, R. J., & Weaver, H. F. 1953, *Statistical Astronomy* (Berkeley and Los Angeles: University of California Press)
- van Altena, W. F., Lee, J. T., & Hoffleit, E. D. 1995, *The General Catalogue of Trigonometric Stellar Parallaxes, Fourth Edition* (New Haven: Yale University Observatory) CDS Strasbourg Data Center Catalog No. I/238A (YPC)
- Zacharias, N., Urban, S. E., Zacharias, M. I., Wycoff, G. L., Hall, D. M., Germain, M. E., Holdenried, E. R., & Winter, L. 2003, *The Second U.S. Naval Observatory CCD Astroglyph Catalog (UCAC2)* (Washington: U.S. Naval Observatory) CDS Strasbourg Data Center Catalog No. I/289
- Zacharias, N., Urban, S. E., Zacharias, M. I., Wycoff, G. L., Hall, D. M., Monet, D. G., & Rafferty, T. J. 2004, *AJ*, 127, 3043

Table 1. Content of the NPM1 and NPM2 Catalogs (stars per field)

Star class	Mag. range (approx.)	NPM1 899 fields	NPM2 347 fields
Faint anonymous stars (FAS)	$(15 < B < 17)$	70–140	~400
Bright anonymous stars	$(10 < B < 13)$	15–30	...
Positional reference stars	$(9 < B < 12)$	~50 ACRS <sup>a</sup>	~400 Tycho-2
Photometric standard stars	$(8 < B < 18)$	0–100	0–100
ICSS “special stars”	$(8 < B < 18)$	~30	~100
Other catalog stars	$(8 < B < 14)$	...	~40 Hipparcos

<sup>a</sup>NPM1 used ACRS catalog data for reference stars originally selected from the AGK3 ( $\delta > -2^{\circ}.5$ ) or SAO ( $\delta < -2^{\circ}.5$ ) catalogs.

Table 2. Lick Astrograph Plate Constant Model<sup>a</sup>

Term	Scale <sup>b</sup>	Rot <sup>c</sup>	Quadratic <sup>d</sup>							Cubic <sup>e,f</sup>				
			Zero Pt		$P_X$	$Q_X$	$P_Y$	$Q_Y$	$D_{1X}$	$D_{2X}$	$D_{1Y}$	$D_{2Y}$	$D_3$	
$c_i$	$c_1$	$c_2$	$c_3$	$c_4$	$c_5$	$c_6$	$c_7$	$c_8$	$c_9$	$c_{10}$	$c_{11}$	$c_{12}$	$c_{13}$	$c_{14}$
$T_{i,X}$	$X$	$Y$	0	1	0	$X^2$	$XY$	0	0	$X^3$	$XY^2$	0	0	$X^2Y$
$T_{i,Y}$	$Y$	0	$-X$	0	1	0	0	$XY$	$Y^2$	0	0	$X^2Y$	$Y^3$	$XY^2$

<sup>a</sup>For NPM2, the same model is used for positions *and* proper motions. The plate center is the origin of the  $X, Y$  coordinates.

<sup>b</sup>One scale term ties the  $X$  and  $Y$  solutions together.

<sup>c</sup>The usual rotation term is split into  $X, Y$  components.

<sup>d</sup>The usual plate tilt terms  $P, Q$  are split into  $X, Y$  components.

<sup>e</sup>The usual cubic distortion term  $X(X^2 + Y^2)$  in  $X$ ,  $Y(X^2 + Y^2)$  in  $Y$  is split into four parts.

<sup>f</sup>The anomalous distortion term  $D_3$  is the same in  $X$  and  $Y$ .

Table 3. Lick NPM2 Catalog: Declination Zone +83°

NPM2	R.A	(J2000)	Dec.	$\mu_\alpha$	$\mu_\delta$	$B$	$B-V$	Epoch	Codes	Tycho-2	ACRS	Hipp
+83.0001	21 35 05.079	+83 04 23.46	0.77	-0.43	11.60	1.57	69.10	2 1 000	4649 02347 1	562334	000000	000000
+83.0002	21 44 18.741	+83 04 42.14	1.61	-0.96	15.11	0.84	69.10	1 1 000	0000 00000 0	000000	000000	000000
+83.0004	21 47 19.602	+83 01 56.60	-3.33	-0.41	11.12	1.44	69.10	2 1 000	4649 02429 1	000000	000000	000000
+83.0005	21 51 14.098	+83 11 32.50	0.13	-0.05	10.55	0.47	69.10	2 1 000	4649 01903 1	563517	000000	000000
+83.0006	21 53 52.852	+83 02 15.28	-0.48	-1.03	16.10	0.59	69.10	1 1 000	0000 00000 0	000000	000000	000000
+83.0007	22 04 29.183	+83 04 25.78	-0.16	0.04	15.37	0.81	69.10	1 1 000	0000 00000 0	000000	000000	000000
+83.0008	22 06 21.215	+83 04 57.76	2.49	-3.03	12.31	0.82	69.10	2 1 000	4650 02792 1	000000	000000	000000
+83.0009	22 14 06.989	+83 11 11.09	-0.22	-0.88	16.63	1.01	69.10	1 1 000	0000 00000 0	000000	000000	000000
+83.0010	22 16 43.463	+83 01 29.07	-0.69	1.34	11.53	1.33	69.10	2 1 000	4650 02484 1	565099	000000	000000
+83.0011	22 24 04.573	+83 11 10.13	-0.20	0.86	15.67	0.88	69.10	1 1 000	0000 00000 0	000000	000000	000000
+83.0012	22 28 05.231	+83 10 31.25	-0.98	-1.22	10.95	0.48	69.10	2 1 000	4650 00738 1	565757	000000	000000
+83.0013	22 33 51.856	+83 07 01.28	-1.23	0.28	14.95	0.95	69.10	1 1 000	0000 00000 0	000000	000000	000000
+83.0014	22 34 41.628	+83 08 24.50	-2.53	-2.01	12.11	0.67	69.10	2 1 000	4650 01631 1	000000	000000	000000
+83.0015	22 38 16.266	+83 00 50.42	-0.64	1.37	11.90	1.10	69.10	2 1 000	4650 00230 1	566296	000000	000000
+83.0016	22 38 33.253	+83 10 00.24	25.75	17.04	14.44	1.57	69.10	4 1 000	0000 00000 0	000000	000000	000000
+83.0017	22 44 21.540	+83 10 08.08	-0.26	0.02	15.63	1.53	69.10	1 1 000	0000 00000 0	000000	000000	000000
+83.0018	22 52 42.965	+83 18 54.85	4.12	4.16	12.07	0.38	69.10	2 1 000	4650 01471 1	000000	000000	000000
+83.0019	22 55 19.344	+83 08 54.31	2.69	2.05	15.59	0.59	69.10	1 1 000	0000 00000 0	000000	000000	000000
+83.0020	22 57 04.531	+83 03 10.02	2.22	1.06	9.31	1.06	69.10	2 1 000	4650 00610 1	000000	113328	000000
+83.0021	23 05 31.480	+83 06 31.71	2.45	-0.36	14.98	0.99	69.10	1 1 000	0000 00000 0	000000	000000	000000
+83.0022	23 18 07.412	+83 00 38.89	-0.67	0.36	11.00	1.39	69.10	6 1 000	4650 01027 1	568200	000000	000000
+83.0023	23 22 05.225	+83 01 52.70	0.53	-1.66	11.56	0.64	69.10	2 1 000	4650 01177 1	000000	000000	000000
+83.0024	23 31 57.330	+83 05 08.36	0.00	-0.36	11.23	1.68	69.10	2 1 000	4650 01108 1	568850	000000	000000

Note. — Table 3 shows the first (and smallest) of the 108 one-degree declination zone files (+83° to -23°) which make up the 232,062-star Lick NPM2 Catalog. This table illustrates the catalog’s format and content. Zones average 2,150 stars; the largest has over 4,200. The machine-readable catalog and full documentation are available at <http://www.ucolick.org/~npm/NPM2> and at the CDS Strasbourg data center (catalog number I/283A). Positions are in the J2000 coordinate system *at the catalog epoch* 2000.0. Proper motion units are arcsec cent<sup>-1</sup>; multiply by 10 for mas yr<sup>-1</sup>. Magnitudes and colors are from NPM2 photographic photometry and the Tycho-2 Catalogue, as explained in Section 6. “Epoch” is the original mean plate epoch for each star. “Codes” are star class, number of fields, and error flags, as explained in the documentation. Tycho-2, ACRS, and Hipparcos numbers are given for NPM2 stars from those catalogs. Other identifications, stellar classifications, and literature references are given in a supplementary catalog, the NPM2 Cross-Identifications.

Table 4. NPM Internal and External Errors<sup>a</sup>

Errors	Position [mas]		Proper Motion [mas yr <sup>-1</sup> ]		Photometry [mag]	
	1968	2000	RMS	Zero Point	$B$	$B - V$
NPM2 internal	77	...	5.6	0.5	0.25	0.25
NPM2 external	84	206	5.9	0.6	0.18	0.20
NPM1 Catalog	150	220	5	2	0.20	0.15

<sup>a</sup>For positions and proper motions, errors in  $\alpha$  and  $\delta$  components are nearly equal; listed values are the mean of the two components.

Note. — Internal errors represent RMS residuals from NPM2 plate reductions. External errors are determined using over 45,000 stars in NPM2 field overlaps. Positions are compared at 1968, near the mean plate epoch, and at 2000, the NPM2 Catalog epoch. Proper motion RMS errors are for individual stars; zero point errors are for individual fields. NPM1 Catalog errors are external errors from Hanson (1997).

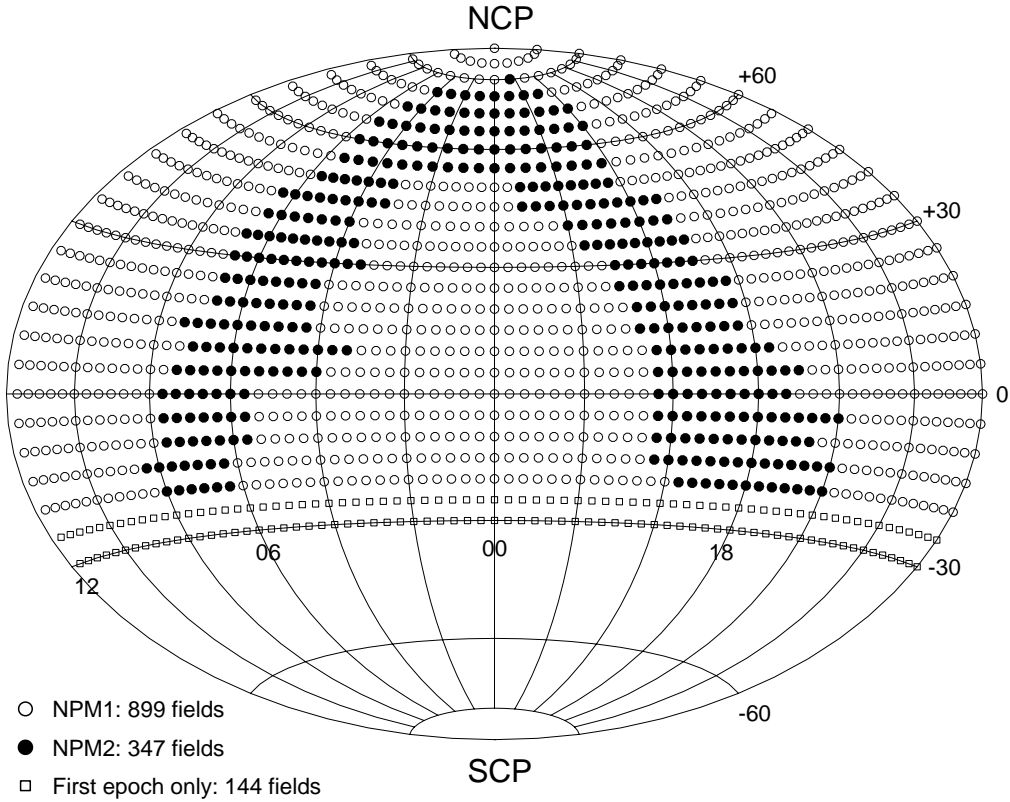


Fig. 1.— Hammer-Aitoff plot showing the distribution of NPM field centers on the sky. Coordinates are B1950 right ascension and declination. The Lick astrograph plates cover  $6^{\circ}.3 \times 6^{\circ}.3$ . Fields are centered in  $5^{\circ}$  declination bands. Right ascension spacing is  $20^m$  ( $5^{\circ}$  at the Equator) for  $|\delta| \leq 35^{\circ}$ , and is progressively adjusted for  $\delta \geq 40^{\circ}$  so that neighboring fields overlap by at least  $1^{\circ}$ . The 1993 NPM1 Catalog comprises 899 fields (open circles) with  $-20^{\circ} \leq \delta \leq +90^{\circ}$  away from the Milky Way. The NPM2 Catalog comprises 347 fields (filled circles) with  $-20^{\circ} \leq \delta \leq +80^{\circ}$  at low galactic latitudes ( $|b| \lesssim 15^{\circ}$ ). Open squares show the 144 “Southern Extension” fields at  $-25^{\circ}$  and  $-30^{\circ}$ , which were photographed at first epoch only, and are not included in the NPM program.

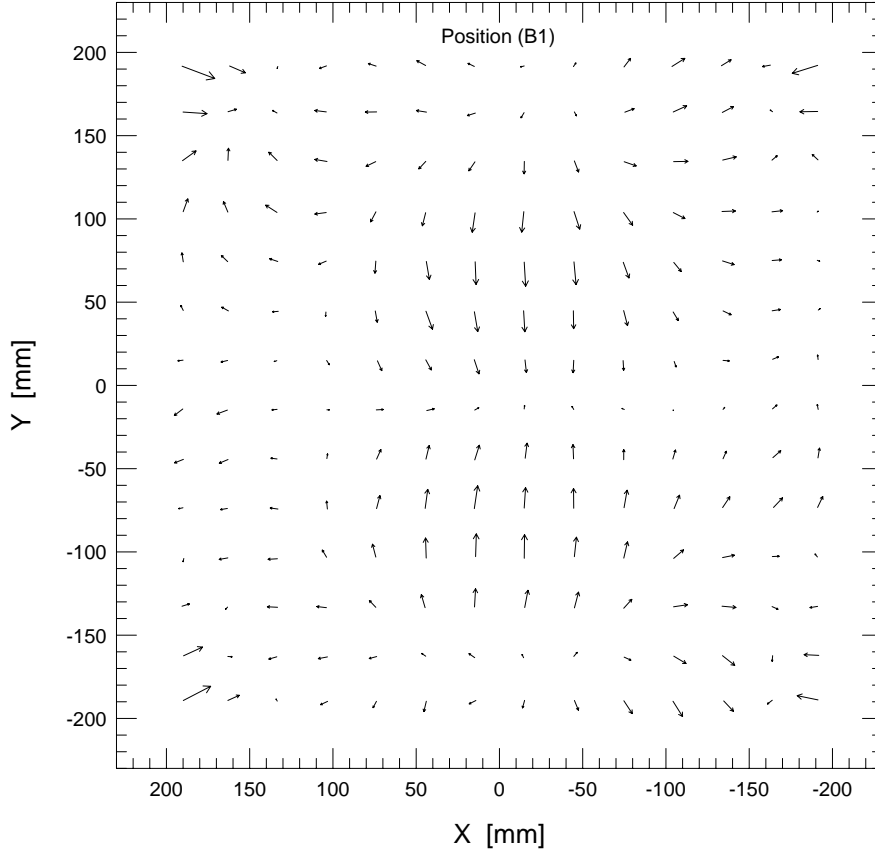


Fig. 2.— Position “mask” for NPM2 first epoch blue plates (B1).  $X, Y$  are Lick plate coordinates. Vectors show the mean residuals  $\langle R_X \rangle$ ,  $\langle R_Y \rangle$  for 122,759 Tycho-2 stars in  $14 \times 14 = 196$  bins (average 626 stars per bin). Vector length scale is  $10 \text{ mm} = 1 \mu\text{m}$ . RMS vector length is  $0.75 \mu\text{m}$  (42 mas). Longest vector is  $2.10 \mu\text{m}$  (116 mas).



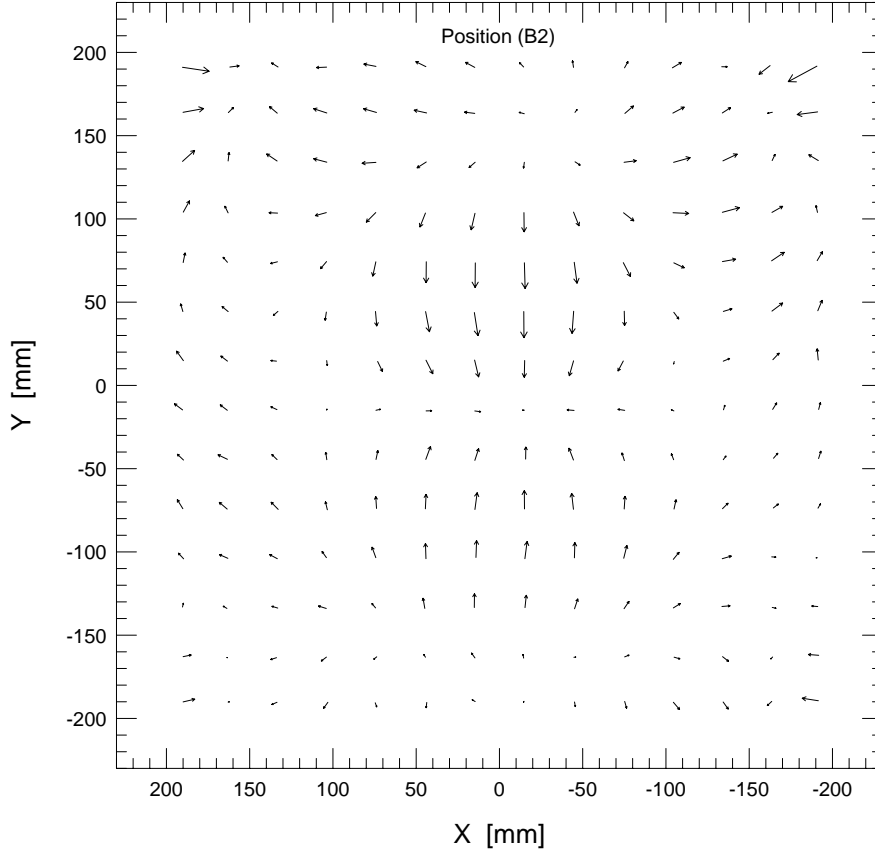


Fig. 3.— Position “mask” for NPM2 second epoch blue plates (B2).  $X, Y$  are Lick plate coordinates. Vectors show the mean residuals  $\langle R_X \rangle$ ,  $\langle R_Y \rangle$  for 118,349 Tycho-2 stars in  $14 \times 14 = 196$  bins (average 604 stars per bin). Vector length scale is  $10 \text{ mm} = 1 \mu\text{m}$ . RMS vector length is  $0.69 \mu\text{m}$  (38 mas). Longest vector is  $1.95 \mu\text{m}$  (108 mas).

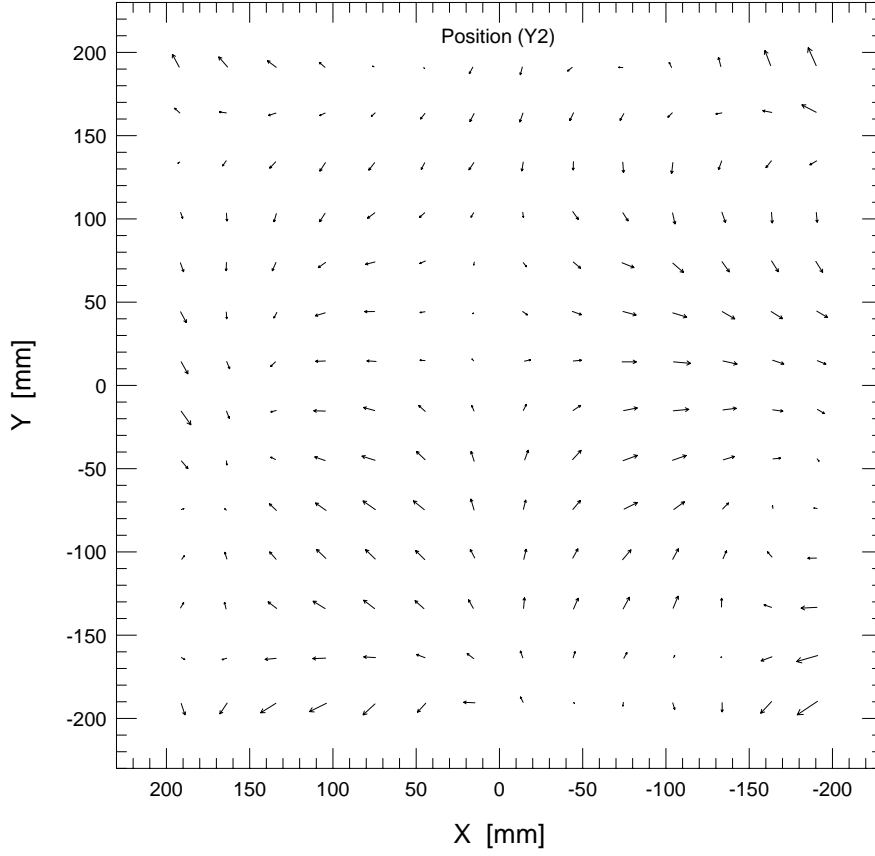


Fig. 4.— Position “mask” for NPM2 second epoch yellow plates (Y2).  $X, Y$  are Lick plate coordinates. Vectors show the mean residuals  $\langle R_X \rangle$ ,  $\langle R_Y \rangle$  for 133,516 Tycho-2 stars in  $14 \times 14 = 196$  bins (average 681 stars per bin). Vector length scale is 10 mm = 1  $\mu$ m. RMS vector length is 0.62  $\mu$ m (34 mas). Longest vector is 1.46  $\mu$ m (80 mas).

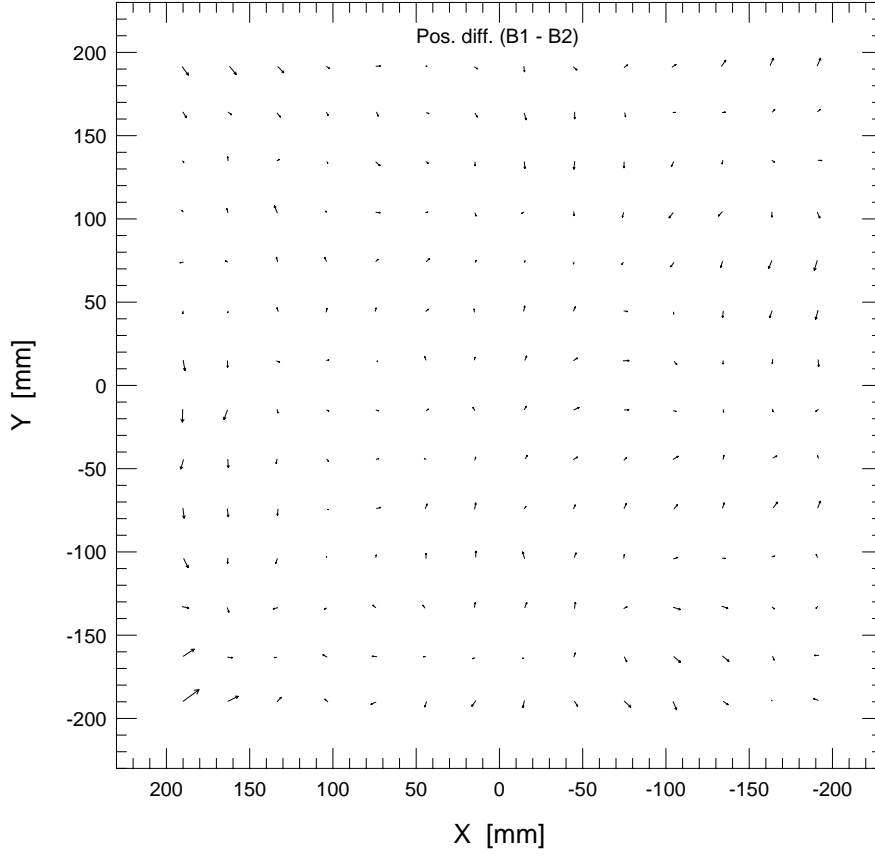


Fig. 5.— Difference “mask” ( $B1 - B2$ ) for NPM2 positions.  $X, Y$  are Lick plate coordinates. Vectors show the differences between the B1 and B2 masks (Figs. 2 and 3) in  $14 \times 14 = 196$  bins. Vector length scale is  $10 \text{ mm} = 1 \mu\text{m}$ . RMS vector length is  $0.33 \mu\text{m}$  (18 mas). Longest vector is  $1.17 \mu\text{m}$  (65 mas). See text for comparison with Figure 6.

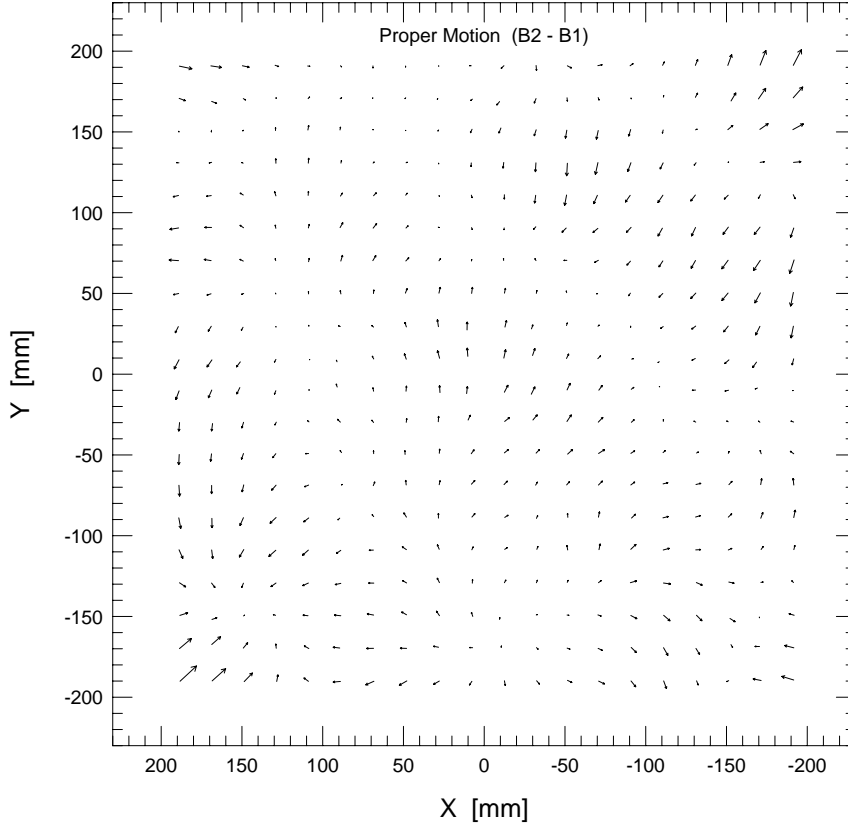


Fig. 6.— “Mask” for NPM2 relative proper motions (B2 – B1).  $X, Y$  are Lick plate coordinates. Vectors show the mean proper motion displacements  $\langle \Delta X \rangle, \langle \Delta Y \rangle$  for 119,954 faint anonymous stars in  $20 \times 20 = 400$  bins (average 300 stars per bin). Vector length scale is  $10 \text{ mm} = 1 \mu\text{m}$ . RMS vector length is  $0.38 \mu\text{m}$  (21 mas). Longest vector is  $1.39 \mu\text{m}$  (77 mas). See text for comparison with Figure 5.